INTERFACE FOCUS

Review

CrossMark
click for updates

Progress and perspectives in signal transduction, actin dynamics, and movement at the cell and tissue level: lessons from *Dictyostelium*

Till Bretschneider[1], Hans G. Othmer[2] and Cornelis J. Weijer[3]

[1]Warwick Systems Biology Centre, University of Warwick, Coventry CV4 7AL, UK
[2]School of Mathematics, University of Minnesota, Minneapolis, MN 55455, USA
[3]School of Life Sciences, University of Dundee, Dundee, UK

TB, 0000-0002-5317-603X; HGO, 0000-0001-6035-5979; CJW, 0000-0003-2192-8150

Movement of cells and tissues is a basic biological process that is used in development, wound repair, the immune response to bacterial invasion, tumour formation and metastasis, and the search for food and mates. While some cell movement is random, directed movement stimulated by extracellular signals is our focus here. This involves a sequence of steps in which cells first detect extracellular chemical and/or mechanical signals via membrane receptors that activate signal transduction cascades and produce intracellular signals. These intracellular signals control the motile machinery of the cell and thereby determine the spatial localization of the sites of force generation needed to produce directed motion. Understanding how force generation within cells and mechanical interactions with their surroundings, including other cells, are controlled in space and time to produce cell-level movement is a major challenge, and involves many issues that are amenable to mathematical modelling.

1. Introduction

Individual cells detect extracellular chemical signals via membrane receptors and mechanical signals via deformation of the membrane or other membrane-mediated mechanisms, and this initiates signal transduction cascades that produce intracellular signals that control movement. Our understanding of signal transduction and motor control in flagellated bacteria such as *Escherichia coli*, who move by swimming and bias their movement by control of their run lengths, is quite advanced [1] compared with our understanding of how amoeboid cells such as macrophages move through tissues. Bacteria sense spatial gradients using a temporal comparison of signals, but larger cells such as macrophages or the cellular slime mould *Dictyostelium discoideum* (Dd) detect differences across their body, and small differences in the extracellular signal over the cell are amplified into large end-to-end intracellular differences. Moreover, cells frequently adapt to the mean extracellular signal level, thereby increasing their sensitivity to signal differences [2,3]. These signals control the motile machinery of the cell and thereby determine the spatial localization of the sites of force generation needed to produce directed motion. When the extracellular signal is a diffusible molecule the process is called chemotaxis, and when the factor is attached to the substrate or extracellular matrix the process is called haptotaxis [4]. Chemotaxis controls the migration towards a source of 3′,5′-cyclic adenosine monophosphate (cAMP) in Dd, and the movement of leucocytes towards attractants released by bacteria in a tissue. Many eukaryotic cells share common mechanisms for sensing and responding to chemoattractant gradients via G-protein-coupled receptors (GPCRs), and to adhesion gradients via integrins or their homologues.

The mechanical interactions of a cell with its environment are mediated by the cytoskeleton, which is a complex network of actin filaments, intermediate

THE ROYAL SOCIETY
PUBLISHING

filaments and microtubules, and associated motor proteins in the cytoplasm. Experimental studies have shown how actin polymerization and network contraction generated by the motor protein myosin lead to force generation within a cell, and have led to detailed maps of actin flow and myosin patterns within certain moving cells. They reveal large regional variations within a cell in the actin network density, and the levels of myosin, nucleation factors, filament binding proteins and other control species that modulate network properties.

The coordination and control of the complex processes involved in direction sensing, amplification of spatial differences in the signal, remodelling of the motile machinery and control of the interaction with the surroundings involves numerous molecules. Their spatial distribution serves to distinguish the 'front' from the 'rear' of the cell, and their temporal expression is tightly controlled. Much is known about the biochemical details of the constituent steps in signalling and force generation, and the focus is now shifting to understanding whole-cell movement. This requires a mathematical model that links molecular-level behaviour with macroscopic observations on forces exerted, cell shape and cell speed, because the large-scale mechanical effects cannot be predicted from the molecular biology of individual steps alone. What is needed are successively more complex model systems that will enable us to test the major modules in an integrated model sequentially, but how to formulate a multiscale model that integrates the microscopic steps into a macroscopic model is a significant challenge in this context.

At sufficiently high densities, as found in a tissue, cell movement is strongly influenced by that of its neighbours. Movement can involve either individual or collective, tissue-like, movement and understanding how the mode of movement is determined may lead to new therapeutic techniques to block tumour metastasis in cancer. Collective movement occurs in the streaming and slug stages of Dd, to be described later. In other cases, cells remain attached to one another, and movement involves massive, coordinated rearrangements of entire tissues, such as folding of the neural plate to form a tube [5,6]. Movement in both cases involves the same processes as for individual cells, with the addition of more-or-less tight coupling between the movement of neighbouring cells, and we refer to both cases as tissue movement.

In this review, we focus on three major groups of processes, thought of as modules, involved in cell motility: (i) signal detection, transduction and direction sensing, (ii) cytoskeletal dynamics, particularly actin dynamics, and (iii) individual and collective cell movement. Throughout we use *D. discoideum* as a model system to illustrate the component processes and their integration during cell or tissue movement. While details of various steps differ between cell types, the major signalling pathways and mechanical processes are highly conserved and thus general principles that emerge from studying Dd will have wide applicability.

1.1. *Dictyostelium discoideum* as a model system

The cellular slime mould *D. discoideum* is widely used as a model system for studying signal transduction, chemotaxis and cell motility. In a favourable environment the free-ranging individual amoebae feed on bacteria and divide by binary fission, but if the food supply is exhausted an elaborate developmental programme is initiated (figure 1). After a period of starvation the cells attain relay competence and can respond to an external cyclic AMP signal by synthesizing and releasing cyclic AMP. After starvation triggers the transition from the vegetative to the aggregation phase, Dd uses cAMP as a messenger for signalling by pacemaker cells to control cell movement in various stages of development [7].

At about 6 h post-starvation the cells begin aggregating in response to periodic waves of cyclic AMP initiated by randomly located pacemaker cells. The production and relay of cAMP pulses by cells that are excitable but not yet oscillatory leads to cAMP waves that propagate outward from a centre and this, coupled with chemotactic movement towards the source of cAMP, facilitates the recruitment of widely dispersed cells (figure 1). In early aggregation the cells move autonomously, but in late aggregation they form connected streams that migrate towards the aggregation centre (reviewed in [7]). At the end of aggregation the cells form a cylindrical slug or grex which may migrate on the substrate for some time. Following migration the slug forms a fruiting body, which consists of an erect stalk that supports a spherical cap containing spores. Under favourable conditions of temperature and humidity the spores are released and can germinate, and the cycle begins anew [8].

Cell motion in Dd consists of the alternating extension of pseudopods and retraction of trailing parts of the cell, but not all extensions are persistent, in that they must anchor to the substrate or to another cell, at least temporarily, in order for the remainder of the cell to follow [9]. Dd cells move relatively rapidly, and contact between the cell and a substrate is via 'close contacts', regions where cell surface glycoproteins bind in a non-specific manner through van der Waals forces [10]. Membrane receptors (Phg1,SadA,SibA) that are involved in substrate adhesion have been identified, but they are much less specific than their mammalian counterparts, which form focal adhesions through specific cell surface receptors called integrins.

In the absence of cAMP stimuli Dd cells extend pseudopods in random directions, probably in order to determine a favourable direction in which to move. Aggregation competent cells respond to cAMP stimuli with characteristic changes in their morphology. The first response is suppression of existing pseudopods and rounding up of the cell (the 'cringe response'), which occurs within about 20 s and lasts about 30 s [11]. Under uniform elevation of the ambient cAMP this is followed by extension of pseudopods in various directions, and an increase in the motility [12]. A localized application of cAMP elicits the cringe response followed by a localized extension of a pseudopod near the point of application of the stimulus [13]. This type of stimulus is similar to what a cell experiences in a cAMP wave. Well-polarized cells are able to detect and respond to shallow chemoattractant gradients of the order of a 2% concentration difference between the anterior and posterior of the cell [2]. Directional changes of a shallow gradient induce reorientation of polarized cells, whereas large changes in the direction of the attractant lead to retraction of a pseudopod and formation of a new one in the direction of the stimulus [14]. Cells also respond to static gradients of cAMP. Fisher *et al*. [15] show that cells move faster up a cAMP gradient than down, and that the majority of turns made by a cell are spontaneous (although there is a slight depression in the frequency of
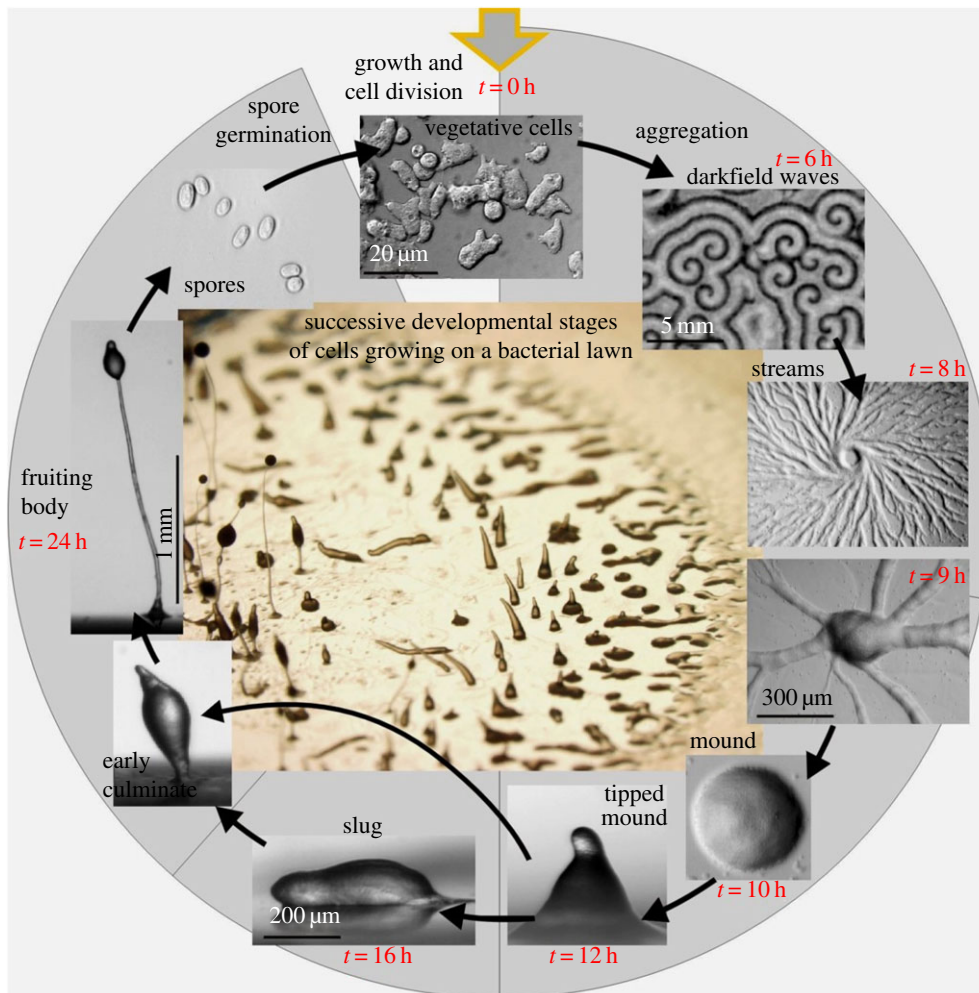
Figure 1. The life cycle of *Dictyostelium*. The central panel shows a *Dictyostelium* colony growing on a bacterial lawn. The images in the outer ring show a close up of various characteristic stages of the life cycle.

turns when the cell moves up the gradient). However, the magnitude and direction of a turn are strongly influenced by the gradient in that there is a strong tendency to lock onto the gradient.

The first step in developing models for the movement of individuals and population-level aggregation patterns is to identify the distinct processes involved in producing the different types of response. What a cell must do can be summarized as follows [16].

— Some cells (or small groups of cells) must become pace-makers. It is known from theoretical studies that a single cell suffices to create an aggregation wave [17], but this has not been demonstrated experimentally.
— A cell must detect the external cAMP and transduce it into an internal signal. A model of this process is discussed later.
— It must choose a direction in which to move and reorganize the cytoskeleton, if needed, to exert the necessary forces for movement.
— Cells must amplify and relay the signal, and adapt to the ambient signal.
— They must respond to an oncoming wave but not to a receding wave, which is called the back-of-the-wave problem.
— Eventually, a cell interacts with its neighbours and moves collectively, first in pairs, then in streams, then in the slug and finally in the erection of the fruiting body.

— During this process it has to 'decide' what type of cell to become in the final fruiting body.
— The entire aggregate has to stop migrating and erect the fruiting body.

In the following sections, we discuss various aspects of signal transduction, actin dynamics, and single and multi-cell movement. In figure 2, we give a preliminary overview of how the processes involved in single cell motility interact before delving into the details.

2. Signal transduction and direction sensing

2.1. Signal transduction

Figure 3a shows the four main pathways involved in transducing an extracellular change in cAMP to a change in the actin network. The central pathway is via Ras, PIP_2, PIP_3 and Rac1, another pathway is through Plc and its products, the third is through guanylate cyclase and the fourth is the cAMP production and secretion/relay pathway through adenylate cyclase. Despite the number of components shown, the diagram not only contains some of the principal actors, and we will not discuss all the components in that diagram in detail, but also those directly involved in the Ras-PIP_2/PIP_3 pathway.

Ras is a member of the Rho family of small GTPases that can be activated by exchange of GDP for GTP. Proteins

cell motility—integrating different mechanisms across scales:
(i) gradient sensing, (ii) cell polarization, (iii) force production and (iv) substrate adhesion
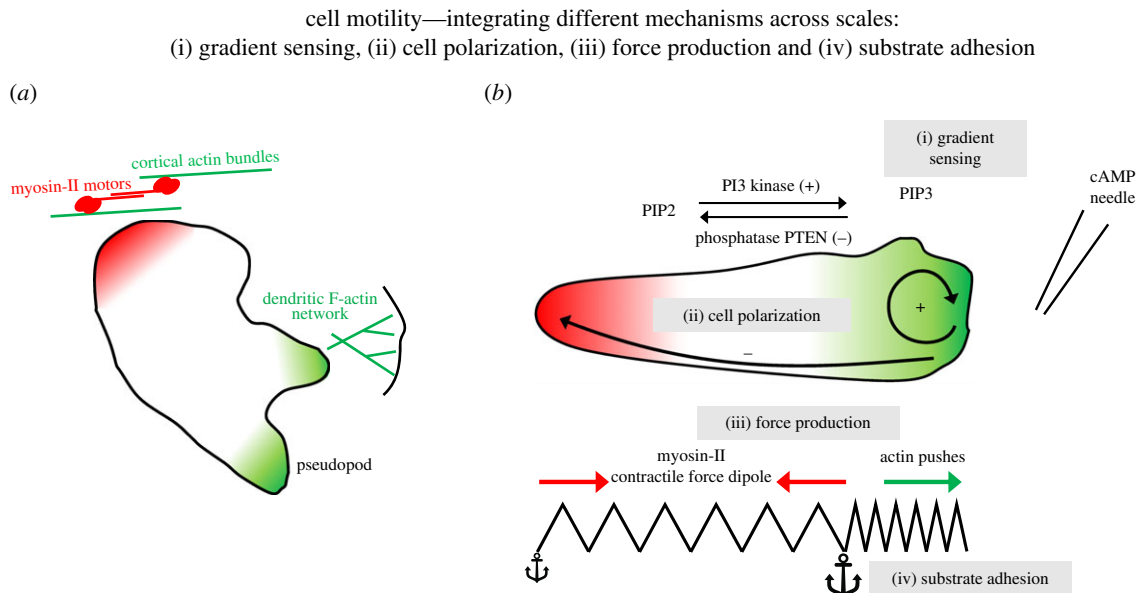

Figure 2. An overview of how the component processes are involved in movement of a cell. (*a*) Random motility. The figure illustrates spontaneous pseudopod formation and front/rear polarization. Growth of a dendritic F-actin network pushes pseudopods forward, whereas myosin-II contractility is responsible for retracting the tail and suppresses pseudopods at the cell rear. The observed patterns in actin and myosin-II are transient. (*b*) Chemotaxis. (i) Positive feedback ($+$) between chemotactic signalling and F-actin helps establishing a stable cell front. (ii) Inhibition ($-$) of front signals at cell rear results in establishing a polarity axis. (iii) The myosin-II contractile force dipole determines the direction of cell motion. Contractile and pushing forces, as well as differential substrate adhesion (iv), all need to be tightly regulated in space and time.
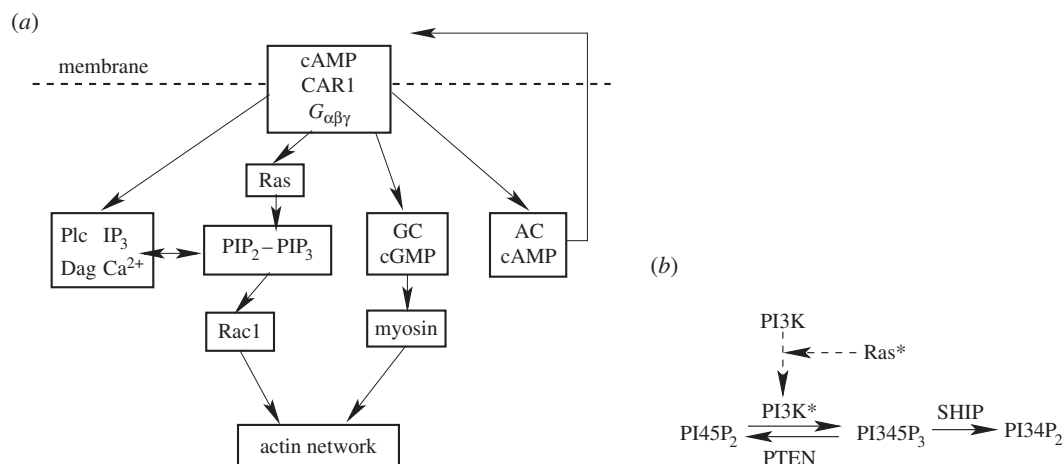

Figure 3. (*a*) Some of the major components of cAMP signal transduction in *Dictyostelium discoideum*. CAR1, the cAMP receptor; $G_{\alpha\beta\gamma}$, a G-protein involved in the transduction of the extracellular signal; Ras, a small G-protein; PIP_2 and PIP_3, components of the membrane that can be interconverted via phosphorylation and de-phosphorylation; IP_3 and DAG, poducts that result from the degradation of PIP_2; Ca^{2+}, calcium; GC, guanylate cyclase—the enzyme that produces cyclic GMP (cGMP); AC, adenylate cyclase—the enzyme that produces cAMP; Rac1, a small G-rotein; myosin, a motor protein involved in contraction of the actin network. (*b*) The PIP_2–PIP_3 trio. Activated Ras activates PI3K, which phosphorylates PIP_2. PIP_3 provides a binding site for cytosolic PI3K, thereby creating a positive feedback loop through PI3K. Similarly, PIP_2 provides a binding site for PTEN, which acts to control PIP_3. PIP_3 levels are controlled in part by PTEN and SHIP, which dephosphorylates PIP_3 at different sites.

in this family are often called molecular switches, as they exist in an active or inactive state and the transition is catalysed by the exchange factors GEF and GAP. However, they function more as adapting rheostats, as the probability of activation reflects the input signal, and the output adapts to a constant signal response.

The first step in the intracellular response to an increase in occupancy of CAR1 is an increase in activated G-proteins. G-proteins consist of an α subunit, G_α that contains a GTP/GDP binding domain as well as intrinsic GTPase activity, and a complex of a G_β and a G_γ subunit. Activation involves exchange of GDP for GTP, followed by dissociation of the α

and $\beta\gamma$ subunits. Each can regulate the activity of different targets in the pathways shown. Both the G_α and $G_{\beta\gamma}$ are involved in activation of the exchange factors for Ras. Following a step increase in cAMP, activated Ras in LatA-treated cells peaks in about 5 s and then adapts (LatA treatment leads to depolymerization of the actin network, which removes any possible feedback effects of downstream components). Experiments show that activation of Ras is also the earliest polarized signalling step downstream of G proteins [18,19].

A subsequent step is the generation of pleckstrin homology-domain binding sites (PHds) by the phosphorylation of the membrane lipid PtdIns(4,5)P_2 (PIP_2) by

phosphoinositide 3-kinases (PI3Ks) to produce PtdIns(3,4,5)P$_3$ (PIP$_3$), which in turn is dephosphorylated to produce PtdIns(3,4)P$_2$ (PIP34P$_2$). Both PIP$_3$ and PI34P$_2$ provide binding sites for various cytosolic proteins such as PI3K, and recruitment is rapid: localization of them at the membrane peaks 5–6 s after global stimulation with cAMP [3,20].

PI3K is activated by Ras* (figure 3) and both PIP$_3$ and PI34P$_2$ are tightly regulated by the phosphatases PTEN and SHIP—within 10–15 s following uniform cAMP changes the PHds return to the cytoplasm [2,3]. This burst of PIP$_3$ at the membrane couples the extracellular signal to actin polymerization via Rac1. The level of activated G-proteins in continuously stimulated cells reaches a stimulus-dependent level, while factors recruited from the cytosol first increase, but then return to basal levels. Therefore, adaptation of the PIP$_3$ and cAMP responses is downstream of G$_{\beta\gamma}$ [21], and it has been shown that adaptation in the PIP$_3$ pathway occurs at the level of Ras [22]. It has also been shown [23] that the increase in PIP$_3$ trails the actin increase in the developing actin waves discussed later, which suggests that there is a feedback from actin to the earlier steps in signal transduction shown in figure 3. Theoretical predictions as to how PI3Ks, PTEN and SHIP are spatially regulated help in understanding how cells respond to changes in the signal [24,25].

Chemotactic signals also produce a rapid, transient, PI3K-dependent activation of Akt/PKB, a protein kinase that is essential for polarization and chemotaxis: mutants lacking Akt/PKB cells cannot polarize properly when placed in a chemotactic gradient and the cells move slowly [26]. Akt/PKB is activated upon recruitment to the membrane, and in Dd it activates the kinase PAKa, which regulates myosin II assembly, cortical tension and retraction of the uropod (the tail) of the cell [3]. PIP$_2$ provides another link between signal transduction and mechanical events in that it acts as a second messenger that regulates the adhesion of the plasma membrane to the underlying cytoskeleton [27].

2.2. Direction sensing and polarization

If the optimal strategy for movement in a noisy chemotactic field is to align with the local gradient, then a cell must determine the direction from a measurement of the local cAMP concentration at its surface, and there are a number of models for how this can be done. Meinhardt [28] postulated an activator–inhibitor model with a third species that serves as a local inhibitor. Amplification of small external differences involves a Turing instability in the activator–inhibitor system, coupled to a slower inactivator that suppresses the primary activation. This model is an interesting high-level description of the process, but lacks a direct mapping onto the biochemistry. It was shown in [29], using a model for the G$_{\beta\gamma}$-AC-cAMP part of the network in figure 3, that a cell experiences a significant difference in the front-to-back ratio of cAMP when a neighbouring cell begins to signal. One could infer from this that other components in the signal-transduction pathway could also show significant front-to-back differences, and this has been demonstrated experimentally for PIP$_3$, PI3K and PTEN. Most current models are based on an activator and inhibitor mechanism similar to that proposed by Meinhardt, called LEGI (local excitation and global inhibition), to explain both direction sensing and adaptation when the chemo-attractant level is held constant [30]. In existing LEGI models, a fast-responding but slowly diffusing activator and

a slow-acting rapidly diffusing inhibitor set up an internal gradient of activity, and while these models shed some light on direction sensing, their usefulness is limited due to the over-simplification of the signal transduction network and the necessity of a wide disparity in the diffusion coefficients of the activator and inhibitor.

The more recent model based on detailed descriptions of the underlying biochemistry can replicate a variety of experimental observations that are not addressed by other models [25]. In particular, it shows that front-to-back symmetry breaking can occur at the level of Ras. This model is based on equal diffusion coefficients for all cytosolic species, and the unbalanced local sequestration of some species leads to gradient sensing and amplification. It is shown that G$_{\alpha_2\beta\gamma}$ cycling between the cytosol and membrane, modulated by Ric-8, a non-receptor GEF for G$_{\alpha_2}$, can account for many of the observed responses in Dd. These include imperfect adaptation, multiple phases of Ras activity in a cAMP gradient and rectified directional sensing that persists over the time scale of a typical wave in aggregation. Thus, this model provides a possible solution to the back-of-the-wave problem that involves only the first steps in the cAMP–G-protein–PIP$_2$/PIP$_3$–actin pathway, but further work is needed, both experimental and theoretical, on the downstream components to determine how they affect the robustness of symmetry breaking.

In general, one can expect that the engineering principles for setting up polarity are very similar in different organisms, but the molecular details can be very different [31]. Another aspect that has not been widely studied concerns the role of noise in detection. Earlier studies show that cells can aggregate successfully even if they make a large error in gradient detection—they only have to orient themselves into the correct half-space in two dimensions—but the aggregation process is slower [32]. Estimates of the signal noise show that it may be important at low signal levels [7], but detailed stochastic simulations of the full reaction–diffusion system are needed to make this more precise.

3. Actin dynamics and the cytoskeleton in the absence and presence of cAMP signals

A central question in cell motility is how a cell generates and controls the forces necessary to produce movement by controlled remodelling and deformation of the cytoskeleton. In the absence of directional signals Dd cells explore their environment randomly, and thus the intracellular biochemical networks that control the mechanics must be tuned to produce signals that generate this random movement. Thus far there is little understanding about how the dynamic rebuilding is controlled, but some insights have been gained by observing the rebuilding of the actin network following treatment with latrunculin A, as is described in this section.

3.1. Plasticity of the actin system in moving cells: creating bundles and networks

Amoeboid cells like Dd owe their overall mechanical integrity to a thin (100–200 nm) intracellular layer of cortical actin adjacent to the cell membrane [33]. This actin cortex, consisting of a loose, cross-linked network of bundled filaments oriented tangentially to the membrane, is highly dynamic and turns-over completely on a time scale of 2 s.
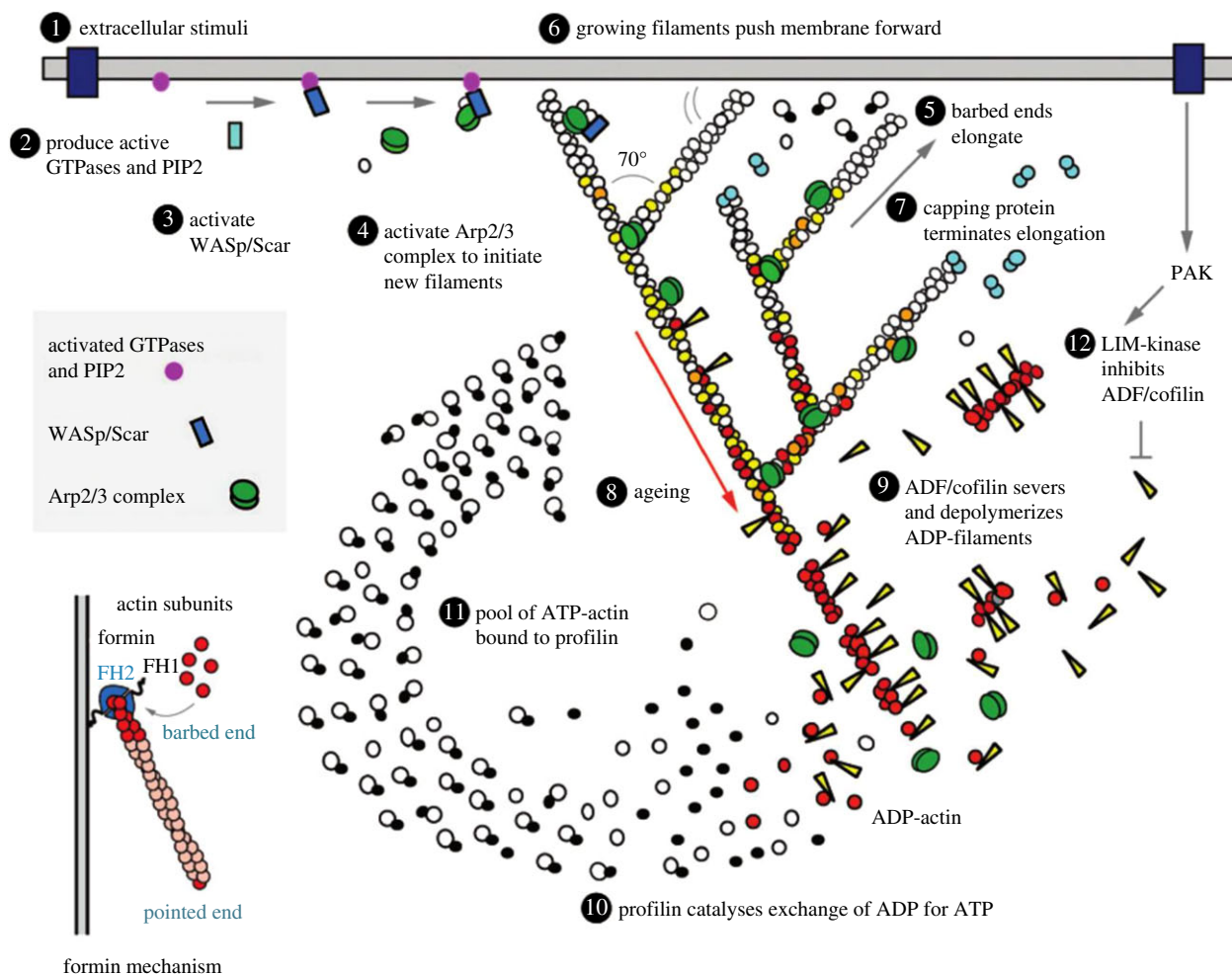
Figure 4. The dendritic actin network, showing some of the major components involved. (From [34], with permission.)

Localized growth of a considerably denser dendritic actin network shown in figure 4 provides the mechanical force driving cellular shape changes, pushing the cell membrane outward in the form of cellular protrusions called pseudopods. Here, the overall orientation of filaments is orthogonal to the membrane. Of course many other factors than actin are involved in deformation of the membrane, including actin cross-linkers, motor proteins and other auxiliary molecules.

The main structural elements of both networks, which underpin the dynamic actin cytoskeleton, are polar filaments of F-actin which originate from the polymerization of monomeric (globular) G-actin, fuelled by adenosine triphosphate ATP. Filaments age by hydrolysis of ATP to adenosine diphosphate (ADP), acting as a timer which primes filaments for disassembly by actin depolymerizing factor (ADF). After nucleation and initial elongation, actin filaments enter a steady-state phase of treadmilling, where the rate at which ATP-actin is incorporated at the growing (barbed) end balances loss of ADP-actin at the opposite (pointed) end. Two major modes of nucleating new actin filaments exist: (i) the formin family of actin nucleators remain associated with the tip of growing filaments while new actin monomers are added. Concurrently, filaments are bundled through fascin cross-linking proteins [35], resulting in actin-cable like structures as observed in the loose matrix of the actin cortex, and also in fine cellular protrusions called filopodia, which contain about 10–30 parallel actin filaments. (ii) The Arp2/3 complex allows branching of new daughter filaments from existing filaments, and is primarily involved in nucleating dense

networks associated with protruding pseudopodia [36]. A host of actin associated proteins exist which are involved in cross-linking, capping filaments to abolish further growth, debranching, severing, depolymerization and the exchange of ADP for ATP to replenish the pool of ATP-actin required for polymerization.

Visualizing actin dynamics in live cells and fine-structural analysis using electron microscopy have been vital to understand the relationship between structure and function in force generation of actin networks. Different probes which consist of the binding domains of F-actin-binding proteins fused to fluorescent proteins, for example green fluorescent protein (GFP), have been constructed to visualize F-actin networks in live cells. Because actin filaments age and networks are constantly remodelled by actin associated proteins, F-actin exists in many different states. Therefore, different probes might only decorate a subset of actin networks and care must be taken when interpreting results. The LimE-coil probe, for example, detects freshly polymerized actin faster than GFP-ABD120 [37]. Lifeact has been suggested as the most reliable probe for detecting most F-actin associated structures in cells [38]. With a diameter of 5–9 nm single actin filaments are well below the resolution limit of light microscopy. Detailed structures of actin networks in cells have recently been obtained by cryo-electron tomography at a resolution of 3 nm [39]. Using correlative microscopy, it is even possible to map high resolution network structures onto live cell images which have been acquired just before freezing and preserving cells.
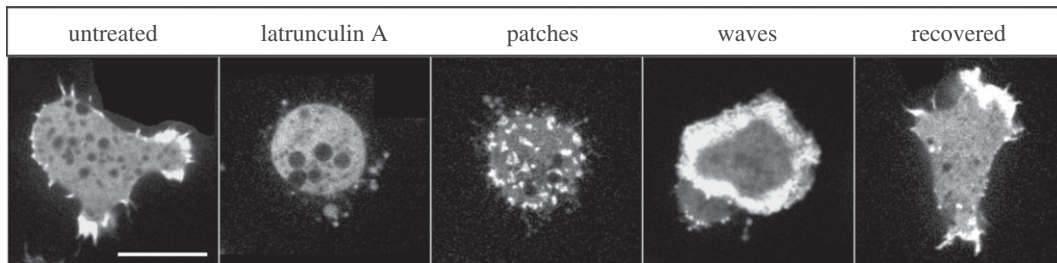
| untreated | latrunculin A | patches | waves | recovered |

Figure 5. The spatial patterns of actin network reorganization after treatment of Dd cells with latA and washout of the drug. The images shown, from left to right, are of a cell moving on a glass surface before the treatment with latA; cells after 16–20 min of incubation with 5 mM latA; patches that appear after the washout of latA; waves appear at a later stage of reorganization before normal cell shape is recovered. Patches are formed within the first 15 min after the removal of latA, waves are most abundant after 20–30 min, and recovered cells are observed after 40 min or longer. The bar is 10 μm, stain is GFP-actin and cells do not translocate in this situation. Approximate times are $T = 0$ min, $T = 20$ min after incubation with 5 mM latrunculin, just before washout. $T = 35$ min patches (approx. 15 min after washout); waves 50 min (approx. 30 min after washout), $T = 60$ min, recovered. (From [37], with permission.)

3.2. *In vitro* polymerization using minimal systems reveals how networks growing in the form of actin comets can generate force

That the growth of an actin network can provide a pushing force was beautifully shown in a series of experiments starting in the 1990s, when it was found that intracellular bacterial parasites like *Listeria monocytogenes* can hijack a cell's actin system [40]. Growth of an actin network on the surface of bacteria, observable in the form of a trailing actin comet, propels pathogens through the host cell and is responsible for spreading from one cell to another. This behaviour can be reconstituted *in vitro* using polystyrene beads coated with an activator of the Arp2/3 complex, and a minimal cocktail containing ATP, actin, Arp2/3 complex, capping proteins, ADF and profilin which catalyses the exchange of ADP for ATP [41].

Recent numerical simulations by Zhu & Mogilner [42] are in good agreement with experimentally observed trajectories of actin-propelled spherical beads. The obtained one-dimensional force velocity relation of the growing actin network is $v = v_0 \exp(-F/Nf_0)$, where v is the average bead velocity acquired by N actin filaments pushing. N is assumed to be approximately 60 for a bead with radius $R = 1$ μm. The scaling factor $f_0 \sim 1.5$ pN is taken as one half of the stall force of 3 pN for an individual filament. $v_0 = 50$ nm s^{-1} is the filaments' zero-load polymerization speed and F is considered to be a constant load. The underlying mesoscopic mathematical model combines two approaches, firstly, the elastic Brownian ratchet model of individual filaments pushing the bead [43] and secondly, a visco-elastic network of interconnected springs describing the actin comet tail as a gel. Macroscopic elastic deformation and stresses which build up in this network also effectively contribute to propulsion of the bead. Interestingly, experiments with ellipsoidal beads that were uniformly coated with an actin nucleation-promoting factor show a bistable orientation where beads are either pushed along the short or long axis, roughly at a ratio of 1 : 1. The elastic deformation model alone favours pushing along the long axis, whereas the individual filament model results in pushing along the short axis. The hybrid model correctly predicts the experimental bistable distribution of bead orientations.

3.3. Actin waves reveal intrinsic excitable properties of the actin system

It suggests itself that the very same mechanism which propels beads and pathogens like bacteria or viruses is at play when it comes to pushing the membrane in moving cells. This is strongly supported by experiments where actin at the front of a moving cell is photobleached. Owing to treadmilling of actin, where newly polymerized actin is inserted at, and pushes the membrane, retrograde flow of the bleached actin towards the cell centre can be observed.

The main question in understanding cell motility is how cells switch actin network growth on or off dynamically. Above all, regulation occurs on the level of membrane associated filament nucleation. Once nucleation of a network has started, Arp2/3 mediated branching will result in autocatalytic growth. Naturally, the time it takes for filaments to age determines the delay before branched growth is inhibited by severing and depolymerization of F-actin. Autocatalytic growth and delayed inhibition are at the core of excitable dynamical systems. Vicker [44] was the first to suggest that the actin system behaves like an excitable system, supported by the existence of actin polymerization waves propagating on top of the inner surface of the cell membrane. In *Dictyostelium* actin waves become prominent during rebuilding of the actin network following treatment with latrunculin A (latA). LatA sequesters G-actin monomers with high affinity and leads to depolymerization of the network. Following washout of latA, the rebuilding of the actin network can be observed using total internal reflection microscopy (TIRF) or three-dimensional confocal microscopy. TIRF targets labelled species within a thin region near the cell–substrate interface (usually less than 200 nm) and thus allows visualization of components near the surface. An example of the evolution in time of the reconstruction of the network is shown in figure 5. The waves shown in this figure only arise at those parts of the cell membrane in contact with a substrate, and thus membrane-surface interaction is essential. Actin structures in the shape of spots initially form on the ventral membrane of the substrate-attached cell, and then propagate radially in roughly circular shape with a prominent wavefront and a decaying wave back [37], as seen in figure 5. Photobleaching experiments show that the wave propagates not via direct transport of existing filaments, but rather, through *de novo* polymerization at the leading edge of the wave and *in situ* depolymerization at the trailing edge [37]. Imaging of the three-dimensional actin waves shows that continual growth of the actin network at the membrane pushes the network upward into the cytoplasm as shown in the schematic in figure 6.

Imaging of labelled components has identified the critical actin-binding proteins involved in network reconstruction
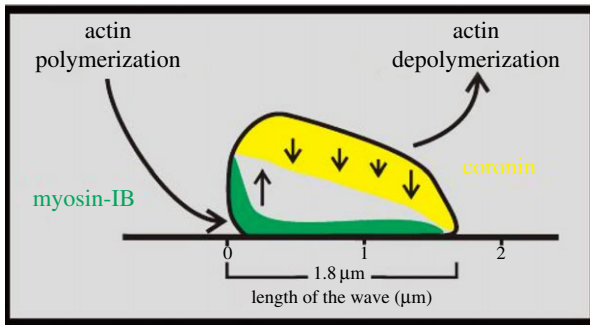
Figure 6. A cross-sectional view of the actin network within a wave, showing net polymerization at the front and net depolymerization at the top and rear. (From [23], with permission.)

[23]. The actin network in the wave is believed to be dendritic, similar to that in actin comets and pseudopodia, due to the high concentration of Arp2/3 complexes measured. The Arp2/3 complex can be activated by binding to nucleation-promoting factors (NPFs), G-actin and existing filaments. This interaction can lead to the formation of new filaments, in which the Arp2/3 complex nucleates daughter filaments branching from a primary filament. In latA-treated Dd cells, myosin-IB (Myo-IB), a single-headed motor molecule that binds to the membrane and to actin filaments in the cortex, is localized at the wavefront, close to the membrane. The scaffolding protein CARMIL is probably recruited to the wavefront by MyoB and activates the Arp2/3 complex. In addition to CARMIL, other NPFs, such as WASP and SCAR [45], may activate Arp2/3. However, NPFs must first be activated on the membrane by binding to phospholipids. It is also observed that coronin, which is bound to filaments at the top and the back of the wave (cf. figure 6), probably destabilizes the network by removing Arp2/3 from a branch junction, thus exposing the pointed end to depolymerization [46]. A suggested schematic of these interactions is shown in figure 7 [23]. There is strong evidence that phospholipid signalling is an integral part of this actin oscillator with a positive feedback loop in which F-actin activates PI3K. PI3K-dependent production of PIP3 phosphoinositides, integral constituents of the cell membrane, can in turn stimulate further F-actin production through Rac, which activates NPFs of Arp2/3 [47,48]. Khamviwath *et al.* [24] have proposed a continuum model for actin waves based on a large number of molecular details of actin network dynamics and the PI3K pathway (figure 7). The model predicts the structure, composition and dynamics of waves in good agreement with experimental data. In addition, it captures a peculiar feature of actin waves, namely the possibility to reverse direction, which cannot easily be explained by standard reaction–diffusion models. Models describing how actin networks and waves interact with deformable cell membranes and can result in protrusive behaviour have been put forward by Enculescu *et al.* [49] and Doubrovinski & Kruse [50]. A considerable number of models are reviewed in [51,52].

Dictyostelium cells in which PIP3 signalling is abolished are still able to move and chemotax [53]. This suggested that actin waves are more likely to play a physiologically relevant role in the PIP3-dependent process of macropinocytosis, the uptake of fluid by cells, where actin coats vesicles that become internalized. However, recently Sun *et al.* [54] show compelling evidence that actin waves do indeed play a role in cell migration. They created structured surfaces with asymmetrically sloped nanoridges. The nanotopgraphy unidirectionally biases internal actin polymerization waves and cells move with the same preferred direction as these waves. These actin waves are observed in the presence of a PI3K inhibitor, and in *Dictyostelium* cells undergoing development, which do not macropinocytose.

3.4. Actin polymerization in response to extracellular signals

In a landmark paper, Parent & Devreotes [2] have shown that cells can sense gradients of chemoattractants even in the absence of an intact actin system. Fluorescently labelled PH-domain proteins which bind to PIP3 phosphoinositides in the membrane were found to face the higher concentration of chemoattractant. A local-excitation global-inhibition mechanism had been proposed to explain the crescent like pattern, similar to what is generally found in Turing-type models for pattern formation. Today, the asymmetric distribution of PIP3 is no longer considered to be the immediate signal responsible for directing actin polymerization in moving cells. Recently, a complex of Elmo/Dock proteins was shown to directly link the $G_{\beta\gamma}$ component of *Dictyostelium* chemoattractant receptors to Rac activation of the actin cytoskeleton during chemotaxis [55]. Lockley *et al.* [56] were able to reduce the Meinhardt model described earlier to two variables and to fit it to experimental data of randomly migrating *Dictyostelium* cells, and cells orienting in a gradient of mechanical shear flow. F-actin fluorescence was used as a read-out of the activator variable. A model by Levchenko & Iglesias [57] fitted the data similarly well, but in its original form is not uniquely identifiable. Both models are minimalistic; however, they assume quite different regulatory mechanisms. In the Meinhardt model, the extracellular signal acts on the activator variable, which in turn promotes production of its own inhibitor. In the Levchenko model, the signal directly acts on the activator and the inhibitor. Given that two different models, both with a comparable number of parameters, explain the experimental data similarly well raises a number of information theory related questions which require some future work. Ideally, one would be able to design experiments which give a well-defined answer, based on different outcomes predicted by numerical simulations or analytical results. In the long run, one would like to integrate more and more molecular details. Although reduced, the Meinhardt model presented in [56] still contains 11 parameters. Increasing the number of parameters inevitably bears the risk of overfitting the data. Regarding the experimental side we must appreciate that, although we might be able to visualize the distribution of a particular molecular component, we hardly ever can determine its exact state, i.e. whether it is active or inactive, bound to another molecule or not, etc.

On the other hand, we can ask what level of molecular detail do we really need to understand in order to predict higher level cellular functions. Excitable systems have the advantage that they provide surprisingly robust mechanisms of pattern formation. Propagating waves can be achieved by a multitude of different models. Examples that gross oversimplification of the internal cellular machinery can still produce meaningful results about cell motility are models where the Meinhardt model has been solved on an evolving boundary [58,59]. The activator concentration is simply translated into a force normal to the cell surface. These models
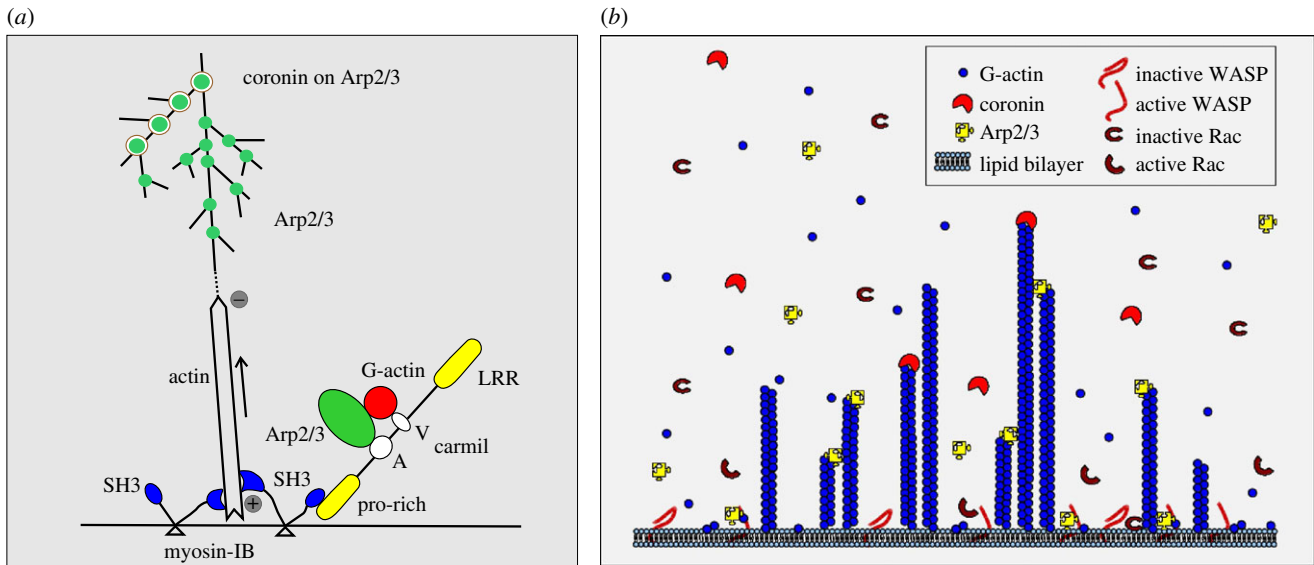
Figure 7. (a) A schematic of a suggested model for actin wave formation. The tail of Myo-IB (blue) binds to the plasma membrane while the motor attempts to move towards the plus end of an actin filament, which maintains attachment of the growing filament to the membrane. The head may also attach to the scaffold protein CARMIL (yellow), which links it to the Arp2/3 complex, where new branches are formed via Arp2/3 binding (green). The activity of the Arp2/3 complex is inhibited by coronin (brown circles). (From [23], with permission.) (b) A schematic of the model for actin waves in [24], wherein model details are given.
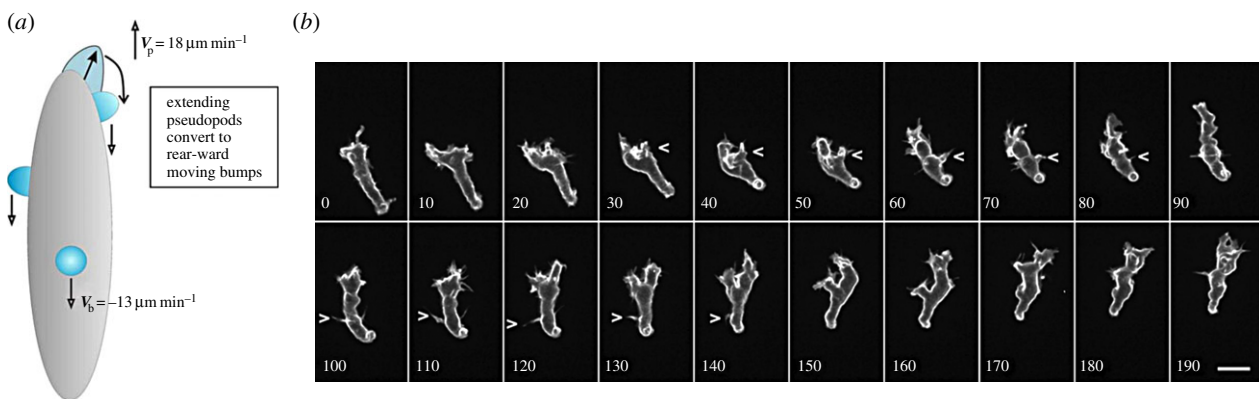

Figure 8. Amoebae swim by protrusions: (a) a swimming cell with three protrusions [64]; (b) the shape of an amoeboid as it swims [63]. Numbers indicate time in seconds. Cells are swimming towards a micropipette releasing cAMP above the top of the frames.

capture a number of non-trivial aspects of cell motility, like the splitting of pseudopods or characteristic cell trajectories, which emerge from the coupling of biochemical pattern generator with a biophysical model of a cell membrane.

4. Single cell and tissue-like movement in *Dictyostelium*

4.1. Swimmers, crawlers and walkers

The movement of crawling cells—those that propel themselves by some form of molecular interaction with the substrate in order to transmit force to the substrate—is classified as either mesenchymal or amoeboid, depending on how the cell interacts mechanically with its environment [60]. The mesenchymal mode is used by cells such as fibroblasts that have a well-organized cytoskeleton, and use strong adhesions to transmit force to their surroundings via integrin-mediated adhesion complexes. Amoeboid motion involves a less structured cytoskeleton and weaker surface interactions, with the result that cells can move much faster

[61]. In this mode cells may use pseudopodia, but can also use protrusions such as blebs, which involve blister-like extensions of the membrane. Dd cells can move either by extending pseudopodia or by blebbing, and they monitor the stiffness of their surroundings to determine the mode: pseudopodia in a compliant medium and blebbing in stiffer media [62]. However, recent experiments show that both neutrophils and Dd can also swim—in the strict sense of propelling themselves through a fluid using only fluid–cell interactions—in response to chemotactic gradients [63,64]. This has led to the suggestion that Dd has three modes of movement—walking, gliding and swimming [64].

In the swimming mode, the cell body is elongated and small protrusions that provide the momentum transfer needed for motion are propagated from front to rear [63,64]. Experimental observations on the movement of Dd cells reported in [63] and [64] have included cell-shape changes, speeds and periods of the cyclic motion. Van Haastert [64] reported an average of three protrusions, as illustrated by the cartoon model in figure 8a, while from the experimental images (figure 8b) of a swimming *Dictyostelium* reported in Barry *et al.* [63], one sees that one protrusion travels along
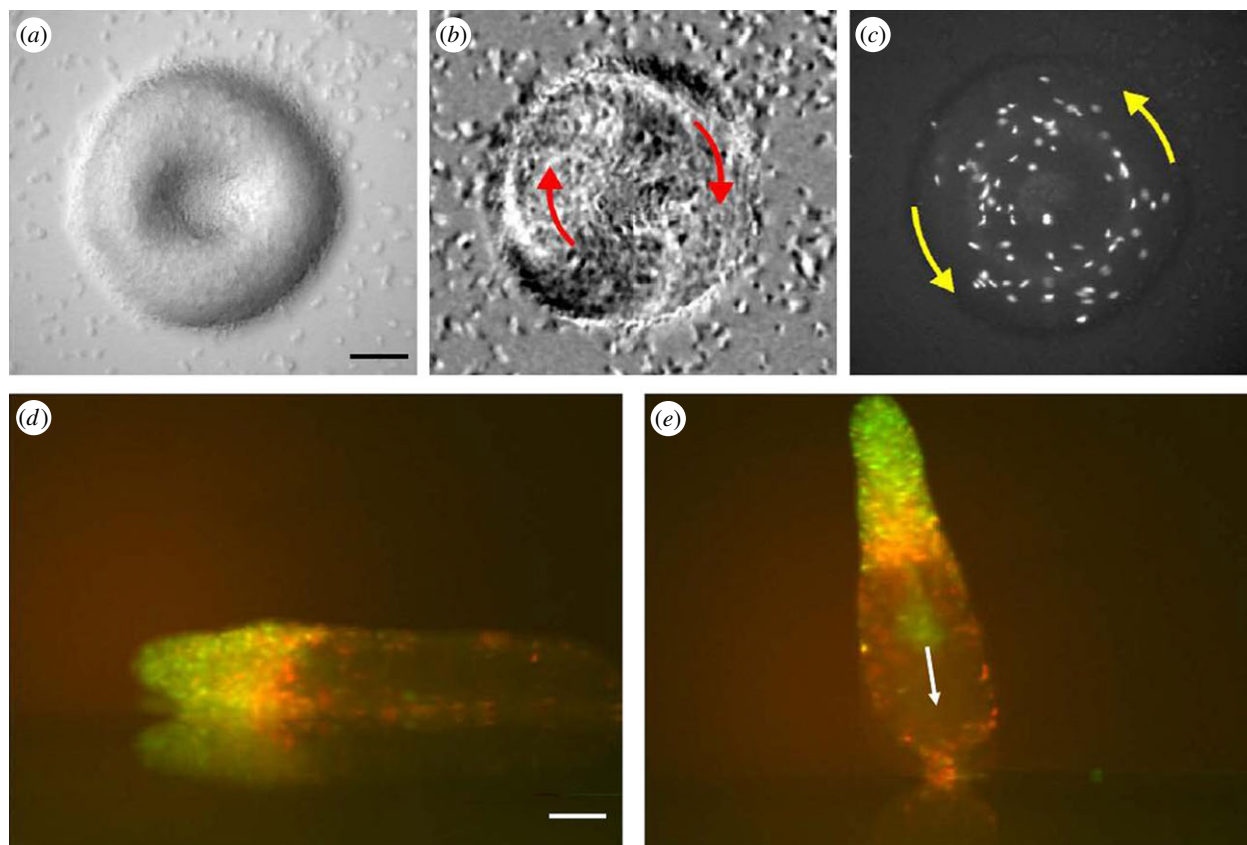
Figure 9. Mound, slug and culmination stages of *Dictyostelium* development. (*a*−*c*) Images of the same mound stage of development processed in different ways to highlight different aspects of mound development. (*a*) Bright field image of mound. (*b*) Image highlighting pinwheel optical density waves rotating clockwise as indicated by red arrows. Waves are visualized by subtraction of two bright field images taken 1 min apart in time. (*c*) Fluorescent image showing 5% GFP labelled cells moving counterclockwise as shown by yellow arrows, in response to waves shown in (*b*). (*d*) Migrating slug; prestalk cells in the tip of the slug express a green GFP marker and anterior like cells located at the prestalk−prespore boundary and scattered in prespore zone express a red GFP marker. (*e*) Image of same slug as shown in (*d*) after it started to culminate. The white arrow indicates the direction of movement of a small mass of green prestalk cells migrating down through the middle of the slug to form the stalk as part of the culmination process. The black scale bar in (*a*) and the white scale bar in (*d*) are 100 μm.

one side of the cell and disappears at the rear of the cell, then another protrusion appears on the other side and repeats the process.

Van Haastert [64] observed that the protrusions travel directly down the cell body and not in a helical fashion. Thus there is no clear evidence that the cell is rotating around its symmetry axis, and as a result a two-dimensional model developed in [65] is a reasonable simplification of a three-dimensional swimming cell. As is shown in figure 8, swimming by extending protrusions is mostly asymmetric in that they alternate sides, and thus the motion is not rotation-free and the trajectory of a swimming cell is snake-like rather than along a straight line. These characteristics of several varieties of swimming Dd amoebae have been reproduced with a computational model [65], and compared with the data described above. The computational model enables one to study how the slenderness of the cell body and the shapes of the protrusion affect the swimming of these cells, and to predict the power consumption and the efficiency of the different varieties.

4.2. Multicellular problems

Collective cell motion occurs in the streaming, mound and slug stages of Dd, as well as in development of vertebrate embryos and cancer metastasis. In Dd streams this involves small numbers of cells, but the slug is composed of about 10^5 to 10^6 cells (cf. figure 9 and [66,67]). The motion of a slug is mechanically very similar to the motion of single cells crawling on a substrate, except that cells in the slug secrete a slime sheath that is essential for the collective movement. The questions that arise in trying to understand how the movement of individuals translates into the collective movement of the slug are the subject of this section.

4.2.1. *Dictyostelium* morphogenesis

Owing to its relative simplicity with only a few cell types in the fruiting body and a relatively simple anatomy, *Dictyostelium* lends itself to trying to understand how relatively well understood cellular behaviours control tissue formation and morphogenesis [66]. A key question is how cell−cell signalling controls cell behaviours to result in emergent properties at the tissue level. As most of multicellular development, aggregation, mound formation, slug formation and migration and the early stages of culmination occur in the absence of significant cell division and cell death it is evident that morphogenesis is the result of differential cell movement of populations of differentiating cells in space and time.

A short description of development (cf. figure 1) is that starving cells aggregate in response to periodic waves of chemoattractant propagating from aggregation centres outward. These periodic waves direct the cells to aggregation centres. Symmetry breaking results in formation of aggregation streams, a process that continues until all cells are collected into hemispherical aggregates known as mounds (figure 9). During aggregation the cells start to differentiate

into several cell types, precursors of the several stalk cell support structures and the spores. The cells going to form the stalk, sort out and form a structure known as the tip. The tip is the organizer that directs the motion of all other cells to form a slug that migrates in response to a variety of environmental signals. During tip formation the prestalk cells start to secrete a complex extracellular matrix known as the slime sheath, which surrounds the mound and the migrating slug like a stocking and is left behind as a slime trail during slug migration. Environmental conditions such as strong light and low humidity trigger the culmination process in which the tip wanders on top of the slug to form the so-called Mexican hat stage. Cells just below the tip start to form a stalk of dead cells, which penetrates the cell mass to contact the cells at the bottom that are going to form the basal disc. The main mass of cells climb up the forming stalk which keeps elongating by successive addition of more stalk cells on the forming stalk (figure 9d,e). This process keeps going until all the cells of the prestalk population are converted into stalk cells as well as supporting structures known as the upper and lower cup that keep the prespore mass in place. Finally, the prespore cells rapidly form individual cells by secretion of spore wall material from prespore vesicles. This is a very rapid process and essentially completes this part of the life cycle. The spores can disperse and start new colonies elsewhere.

4.2.2. Aggregation

It is well established that *Dictyostelium* cells aggregate in response to cAMP signals and much work is concerned with the mechanism of signal detection and translation of graded information along the length of the cell in direction motion by differential organization of the actin myosin cytoskeleton [68,69]. There are various theories about how this may work [59,70]. The cells not only respond to cAMP by moving, but can amplify detected cAMP signals resulting in a cAMP relay mechanism [22,71–73]. This has been modelled extensively [74,75]. The cAMP relay mechanism coupled to diffusion of the signal in the extracellular medium results in formation of various complex wave-forms such as target patterns and spirals, reminiscent of the patters seen in excitable chemical systems such as the Belousov–Zhabotinsky reaction [76]. In *Dictyostelium*, these waves were initially detected as waves of light scattering associated with the locally synchronized chemotactic movement of cells during the rising phase of the cAMP waves [77–80] (figure 1). The *Dictyostelium* process is, however, more complex and interesting than the Belousov–Zhabotinsky reaction as the discrete sources of the signals, the cells, move in response to these waves. This extra dynamics results in much more complex behaviours such as bifurcating stream formation. These processes have been modelled to a great extent and the main features are understood in some considerable detail [32,81–86] (figure 10).

Initially, the cAMP waves were measured in fixed time points using an ingenious isotope dilution strategy, but more recently it has been possible to measure the cAMP waves dynamically using dedicated FRET constructs [87,88]. Interesting questions that can now be started to be resolved are what is the exact mechanism of cAMP amplification in single cells? How heterogeneous is the response of the individual cells and how does this heterogeneity affect the outcome of the overall process? Another interesting question is how the cell signalling proceeds in streams where cells are highly elongated and make extensive end to end cell–cell contacts [89]. It has

been argued that cells produce and secrete cAMP in a polarized manner affecting the mode and speed of signal propagation [90]. In these stages of development there is a considerable Doppler effect and it may be that the speed of movement is controlled by the rate of signalling as the cells cannot move faster than the desensitization time [91].

Forces have been measured using traction force microscopy and it is evident that cells are force dipoles in line with the organization of the cytoskeleton. Cells also need to coordinate their motion in streams which involves coordination of the cytoskeleton in neighbouring cells resulting in local force coordination [44,92–95].

4.2.3. Sorting in the slug

Once the cells enter the aggregates the cells start to sort out. It has been proposed that cell sorting results from differential cell–cell adhesion and there are some experiments to suggest that differential adhesion may play a role in *Dictyostelium* cell sorting. The nature of these adhesion sites is still under debate and ranges from cadherin type molecules to a unique multigene family of large transmembrane signalling molecules involved in self–non-self recognition [96–98]. However, it is clear that cell sorting in *Dictyostelium* involves differential chemotaxis to cAMP [99–101]. A main question is whether cells move differentially as a result of differential sensitivity to cAMP, a differential adhesion resulting in effective differential movement speeds or that the prestalk cells that sort out produce more force and push the other cells aside. There are a variety of experiments that suggest that cells defective in the actin–myosin cytoskeleton cannot sort effectively, suggesting that cell sorting maybe the result of differential motive force generation by the sorting cells. There is evidence for a key role for myosin in the sorting process [102–104].

The cell sorting process is accompanied by a change in the geometry of the signals in the mounds; they often spontaneously go from being single spirals to multi-armed spirals and pinwheel like structures in mounds. This is probably related to the differential ability of cells to produce cAMP in an excitable manner. Data suggest that the adenylyl cyclase that makes cAMP during aggregation becomes restricted to the prestalk cells and so-called anterior like cells during aggregation [105]. It has been proposed that this results in a change of wave geometry from scroll waves in the tip to planar waves in the back of the slug, expanding the observed motion of cells in the slug [106,107]. An alternative view is that the rotational motion observed is due to a drive of the cells to move continuously in a constrained environment, resulting in the observed rotational motion. However, experiments with a temperature sensitive ACA have shown that slug migration is directly dependent on ACA activity [108].

It has also become clear that the slime sheath is an important component during *Dictyostelium* morphogenesis. Some of the key prestalk specific expressed genes code for components of the extracellular matrix, which is a complex composite of proteins and cellulose [109,110]. Cells taken from slugs are not able to move on a glass substrate any more while pre- and aggregation stage cells can. The cells form specific contacts with the matrix through as yet unspecified adhesion molecules. They form, however, transient focal adhesions as exemplified by the formation of transient paxillin spots and deletion of paxillin as well as of talin results in defect of later morphogenesis [111,112].
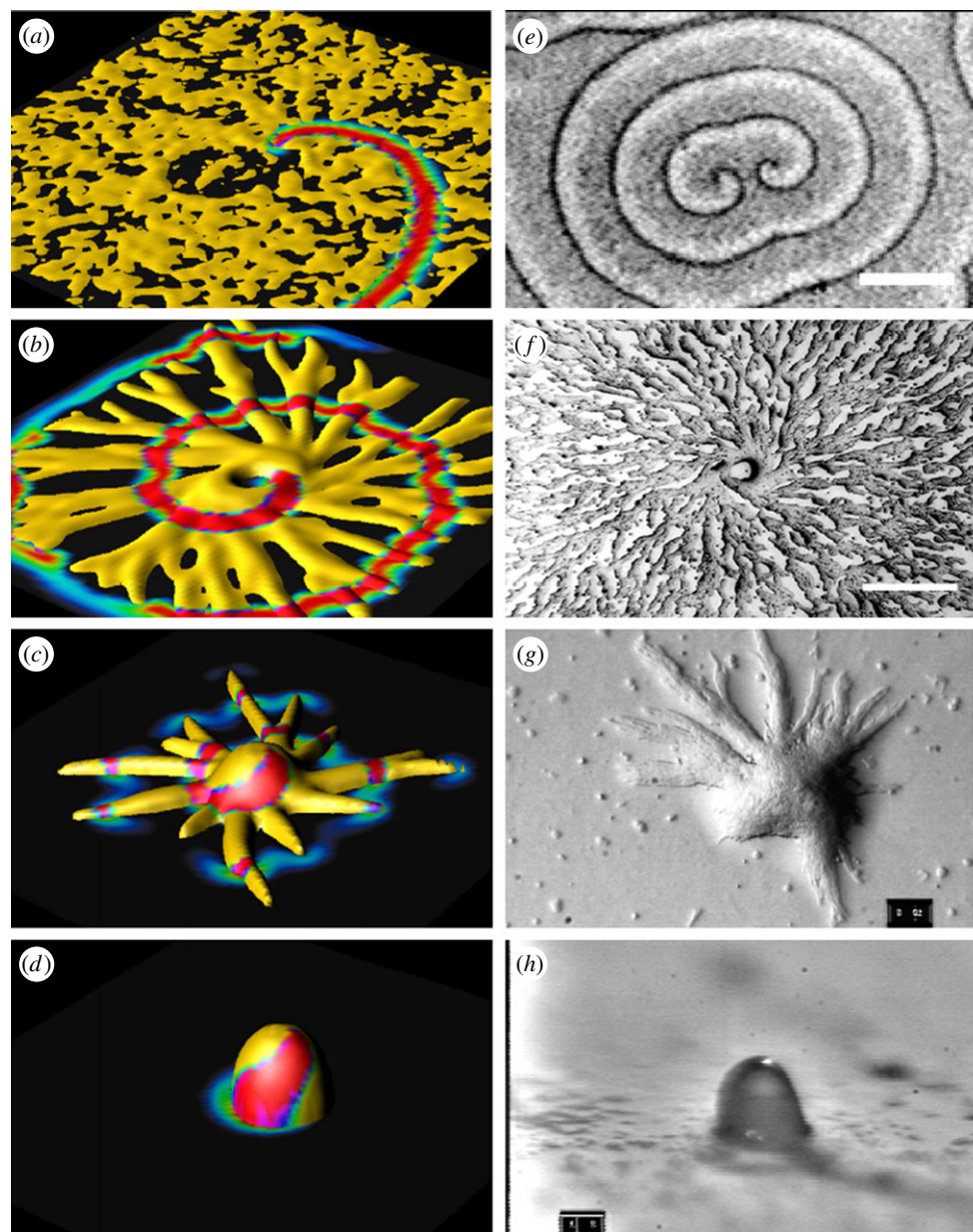
Figure 10. Comparison of simulation of continuous fluid-based model for aggregation and mound formation with stage-matched images of aggregation and mound stages. (a–d) Results of simulations. (e–h) Corresponding experimental stages. Yellow colour represents tissue, red-blue colours the spiral cAMP wave controlling chemotactic tissue movement (from [78]). White scale bars in (e,f) are 450 μm.

Traction force experiments on slugs have shown that the slime sheath plays an important role in the migration of the slug and also have indicated that the prestalk zone maybe be especially important in the generation of motive force [113–115]. In general, it is an open question how the cells in the slug get their traction for movement [116]. Experiments have shown that cells in the slug can move forward relative to other cells, but essentially use other cells as substrate to move on, and for this to work the cellular scaffold has to be relatively stiff. This implies that cells transmit their motive forces through the other cells to the extracellular matrix and that cell–cell adhesion must be an important component in coupling the cytoskeletons of cells (figure 11). This mode of movement effectively leads to the generation of local body forces which have been the basis for various continuous and discrete models for slug migration [117,118]. So far, these models have ignored the role of the slime sheath in this process which will need to be addressed in further work.

4.2.4. Culmination

The culmination process is highly complex; the initial movement of the tip on top of the Mexican hat structure involves differential movement of cells in various transverse positions of the slug. The upper cells stop moving while cells in contact with the substrate move underneath, resulting in the tip relocating to the top and centre of the structure. This then starts a stalk-forming process directed downward, resulting in the formation of the basal disc, stalling fusion and successive elongation of the stalk [119] (figures 1 and 9). It has been suggested that the spore mass is lifted up the stalk by the combined crawling action of the lower- and upper-cup cells [120]. There has been one detailed model of culmination based on the cellular Potts model that captures some of the essential elements [121,122], but many questions, especially the role of cellular and tissue mechanics in this process, remain unresolved.

The final challenge is to integrate the well-known homeostatic cell-type proportioning with the extensive cell movement
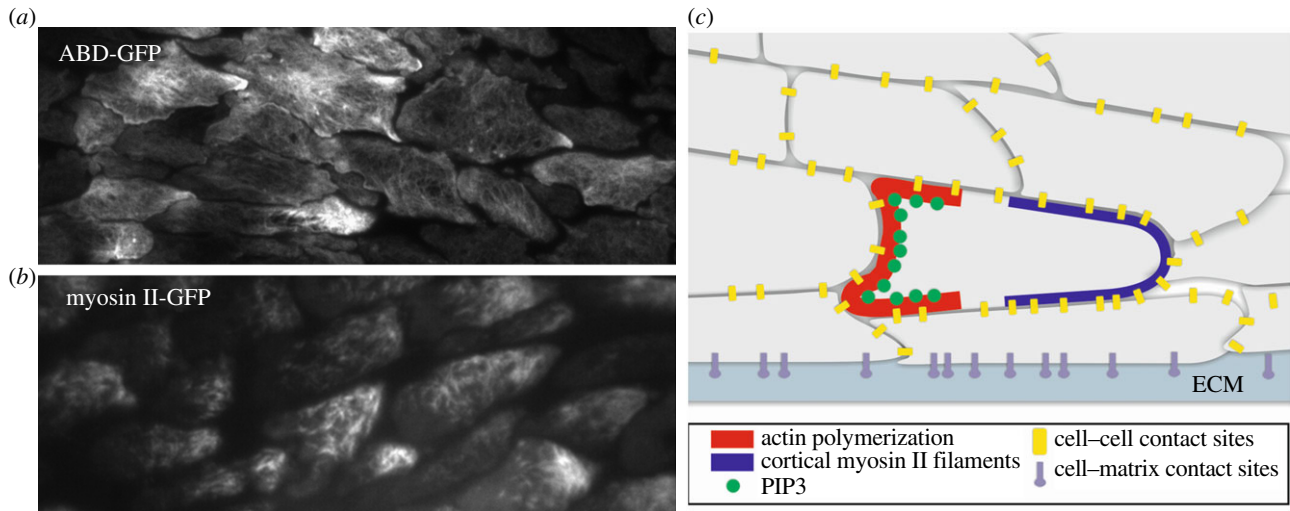
Figure 11. Processes directing cell migration in multicellular stages of Dd. (*a,b*) TIRF images of bottom layer of migrating cells in a slug migrating from right to left. (*a*) Distribution of actin as visualized by ABD120-GFP; note the localization of extensive actin networks in the front and the back of the migrating cells. (*b*) Myosin II as visualized by myosin II heavy chain-GFP; note the localization of myosin II thick filaments in the back of the migrating cells. (*c*) Cross section through slug showing cell−cell and cell−substrate interactions through specific distinct classes of adhesion molecules. One highlighted cell shows polarization of signalling (PIP3) and the actin−myosin cytoskeleton. White scale bars in (*a,b*) are 5 μm.

taking place during development. In the slug, the major prestalk and prespore cell types are spatially separated. The prestalk cells sit in the front and the back and the prespore cells in the middle, with only a scattering of so-called anterior-like cells [123]. Slugs can rapidly and greatly change their shape, while maintaining their cell-type distribution and proportioning [124]. This appears to make it unlikely that differentiation is controlled by gradients of diffusible molecules as has often been proposed for this and other systems. One solution is to regulate the differentiation by local interactions at a cell-type interface once the proportions are established. Another solution would be to couple the cell-type differentiation to the propagating cAMP signal in combination with a long range diffusible substance [125,126].

5. Conclusion

Dictyostelium has provided a rich source of questions from the level of subcellular and cellular molecular mechanisms to the integration of cell behaviours to achieve homeostatic cell differentiation and integration of the cells in complex morphological structures. Modelling has had a big impact on the development and integration of knowledge at the subcellular and cellular level, and has also played an important role in understanding some of the key principles underlying essential parts of multicellular morphogenesis. There are many key unanswered questions where combined experimental and theoretical work will be needed to resolve many of the remaining complex open questions. A number of them are listed below, but the reader will surely have raised many more.

— How can we validate biochemically more detailed models for signal transduction given that usually only a small subset of species/states can be observed?
— Limited spatial and temporal resolution in live cell microscopy results in convolved (blurred) images of the underlying stochastic processes. How can we infer the underlying noise, and can we justify the common use of continuum models?

— How do mechanical signals like membrane tension, which are known to play important roles but largely ignored in mathematical models, feedback on cell migration? How do mechanical coupling and force transmission between cells influence collective cell migration?
— Which signals control differentiation and a variety of cell behaviours and how are these integrated?
— What roles do the various cell types play in morphogenesis?
— What is the role of the extracellular matrix in mechanics of slug migration and culmination?
— What are the major cellular mechanisms underlying cell critical behaviours such as individual and multicellular migration?
— How can we formulate realistic models of cell movement that integrate the processes described herein and yet remain testable and computationally feasible?
— How can mathematical models be used to understand the role of different pathways involved in movement and how are they balanced to ensure a successful outcome at the cell and population level?

It is fair to say that *Dictyostelium* is the organism where most progress has been made in understanding pattern formation and morphogenesis outside plants, and one can expect that this will continue in the near future. As to the role of mathematical modelling in understanding these processes, John Bonner summarized it best long ago [127].

> We have arrived at the stage where models are useful to suggest experiments, and the facts of the experiments in turn lead to new and improved models that suggest new experiments. By this rocking back and forth between the reality of experimental facts and the dream world of hypotheses, we can move slowly towards a satisfactory solution of the major problems of developmental biology.

References

1. Xin X, Othmer HG. 2012 A trimer of dimers-based model for the chemotactic signal transduction network in bacterial chemotaxis. *Bull. Math. Biol.* **74**, 2339–2382. (doi:10.1007/s11538-012-9756-7)

2. Parent CA, Devreotes PN. 1999 A cell's sense of direction. *Science* **284**, 765–770. (doi:10.1126/science.284.5415.765)

3. Chung CY, Funamoto S, Firtel RA. 2001 Signaling pathways controlling cell polarity and chemotaxis. *Trends Biochem. Sci.* **26**, 557–566. (doi:10.1016/S0968-0004(01)01934-X)

4. Alberts B, Johnson A, Lewis J, Raff M, Roberts K, Walter P. 2002 *Molecular biology of the cell*, 4th edn. New York, NY: Garland Science.

5. Davidson LA, Keller RE. 1999 Neural tube closure in *Xenopus laevis* involves medial migration, directed protrusive activity, cell intercalation and convergent extension. *Development* **126**, 4547–4556.

6. Wallingford JB, Niswander LA, Shaw GM, Finnell RH. 2013 The continuing challenge of understanding, preventing, and treating neural tube defects. *Science* **339**, 1222002. (doi:10.1126/science.1222002)

7. Othmer HG, Schaap P. 1998 Oscillatory cAMP signaling in the development of *Dictyostelium discoideum*. *Comments Theor. Biol.* **5**, 175–282.

8. Bonner JT. 1967 *The cellular slime molds*. Princeton, NJ: Princeton University Press.

9. Soll DR. 1995 The use of computers in understanding how animal cells crawl. *Int. Rev. Cytol.* **163**, 43–104. (doi:10.1016/S0074-7696(08)62209-3)

10. Tarantola M, Bae A, Fuller D, Bodenschatz E, Rappel W-J, Loomis WF. 2014 Cell substratum adhesion during early development of *Dictyostelium discoideum*. *PLoS ONE* **9**, e106574. (doi:10.1371/journal.pone.0106574)

11. Condeelis J, Bresnick A, Demma M, Dharmawardhane S, Eddy R, Hall AL, Sauterer R, Warren V. 1990 Mechanisms of amoeboid chemotaxis: an evaluation of the cortical expansion model. *Dev. Genetics* **11**, 333–340. (doi:10.1002/dvg.1020110504)

12. Wessels D, Murray J, Soll DR. 1992 Behavior of *Dictyostelium* amoebae is regulated primarily by the temporal dynamic of the natural cAMP wave. *Cell Motil. Cytoskelet.* **23**, 145–156. (doi:10.1002/cm.970230207)

13. Swanson J, Taylor DL. 1982 Local and spatially coordinated movements in *Dictyostelium discoideum* amoedae during chemotaxis. *Cell* **28**, 225–232. (doi:10.1016/0092-8674(82)90340-3)

14. Gerisch G. 1982 Chemotaxis in *Dictyostelium*. *Annu. Rev. Physiol.* **44**, 535–552. (doi:10.1146/annurev.ph.44.030182.002535)

15. Fisher PR, Merkl R, Gerisch G. 1989 Quantitative analysis of cell motility and chemotaxis in *Dictyostelium discoideum* by using an image processing system and a novel chemotaxis chamber providing stationary chemical gradients. *J. Cell Biol.* **108**, 973–984. (doi:10.1083/jcb.108.3.973)

16. Othmer HG. 2016 *Cell-based, continuum and hybrid models of tissue dynamics*. *Lecture notes in mathematics*. Berlin, Germany: Springer.

17. DeYoung G, Monk PB, Othmer HG. 1988 Pacemakers in aggregation fields of *Dictyostelium discoideum*. Does a single cell suffice? *J. Math. Biol.* **26**, 486–517. (doi:10.1007/BF00276057)

18. Sasaki AT, Chun C, Takeda K, Firtel RA. 2004 Localized Ras signaling at the leading edge regulates PI3K, cell polarity, and directional cell movement. *J. Cell Biol.* **167**, 505–518. (doi:10.1083/jcb.200406177)

19. Charest PG, Firtel RA. 2006 Feedback signaling controls leading-edge formation during chemotaxis. *Curr. Opin. Genet. Dev.* **16**, 339–347. (doi:10.1016/j.gde.2006.06.016)

20. Iijima M, Huang YE, Devreotes P. 2002 Temporal and spatial regulation of chemotaxis. *Dev. Cell* **3**, 469–478. (doi:10.1016/S1534-5807(02)00292-7)

21. Janetopoulos C, Jin T, Devreotes P. 2001 Receptor-mediated activation of heterotrimeric G-proteins in living cells. *Science* **291**, 2408–2411. (doi:10.1126/science.1055835)

22. Takeda K, Shao D, Adler M, Charest PG, Loomis WF, Levine H, Groisman A, Rappel W-J, Firtel RA. 2012 Incoherent feedforward control governs adaptation of activated Ras in a eukaryotic chemotaxis pathway. *Sci. Signal.* **5**, ra2. (doi:10.1126/scisignal.2002413)

23. Bretschneider T, Anderson K, Ecke M, Müller-Taubenberger A, Schroth-Diez B, Ishikawa-Ankerhold HC, Gerisch G. 2009 The three-dimensional dynamics of actin waves, a model of cytoskeletal self-organization. *Biophys. J.* **96**, 2888–2900. (doi:10.1016/j.bpj.2008.12.3942)

24. Khamviwath V, Hu J, Othmer HG. 2013 A continuum model of actin waves in *Dictyostelium discoideum*. *PLoS ONE* **8**, e64272. (doi:10.1371/journal.pone.0064272)

25. Cheng Y, Othmer HG. 2016 A model for direction sensing in *Dictyostelium discoideum*: Ras activity and symmetry breaking driven by a $G_{\beta\gamma}$-mediated, $G_{\alpha2}$-Ric8-dependent signal transduction network. *PLoS Comput. Biol.* **12**, e1004900. (doi:10.1371/journal.pcbi.1004900)

26. Meili R, Ellsworth C, Lee S, Reddy TB, Ma H, Firtel RA. 1999 Chemoattractant-mediated transient activation and membrane localization of akt/PKB is required for efficient chemotaxis to cAMP in *Dictyostelium*. *EMBO J.* **18**, 2092–2105. (doi:10.1093/emboj/18.8.2092)

27. McLaughlin S, Wang J, Gambhir A, Murray D. 2002 PIP_2 and proteins: interactions, organization and information flow. *Ann. Rev. Biophys. Biomol. Struct.* **31**, 151–175. (doi:10.1146/annurev.biophys.31.082901.134259)

28. Meinhardt H. 1999 Orientation of chemotactic cells and growth cones: models and mechanisms. *J. Cell Sci.* **17**, 2867–2874.

29. Dallon JC, Othmer HG. 1998 A continuum analysis of the chemotactic signal seen by *Dictyostelium discoideum*. *J. Theor. Biol.* **194**, 461–483. (doi:10.1006/jtbi.1998.0766)

30. Tang M, Wang M, Shi C, Iglesias PA, Devreotes PN, Huang CH. 2014 Evolutionarily conserved coupling of adaptive and excitable networks mediates eukaryotic chemotaxis. *Nat. Commun.* **5**, 5175. (doi:10.1038/ncomms6175)

31. Thompson BJ. 2013 Cell polarity: models and mechanisms from yeast, worms and flies. *Development* **140**, 13–21. (doi:10.1242/dev.083634)

32. Dallon JC, Othmer HG. 1997 A discrete cell model with adaptive signalling for aggregation of *Dictyostelium discoideum*. *Phil. Trans. R. Soc. Lond B* **352**, 391–417. (doi:10.1098/rstb.1997.0029)

33. Bretschneider T, Diez S, Anderson K, Heuser J, Clarke M, Müller-Taubenberger A, Köhler J, Gerisch G. 2004 Dynamic actin patterns and Arp2/3 assembly at the substrate-attached surface of motile cells. *Curr. Biol.* **14**, 1–10. (doi:10.1016/j.cub.2003.12.005)

34. Pollard TD. 2007 Regulation of actin filament assembly by Arp2/3 complex and formins. *Annu. Rev. Biophys. Biomol. Struct.* **36**, 451–477. (doi:10.1146/annurev.biophys.35.040405.101936)

35. Schirenbeck A, Bretschneider T, Arasada R, Schleicher M, Faix J. 2005 The diaphanous-related formin dDia2 is required for the formation and maintenance of filopodia. *Nat. Cell Biol.* **7**, 619–625. (doi:10.1038/ncb1266)

36. Pollard TD, Borisy GG. 2003 Cellular motility driven by assembly and disassembly of actin filaments. *Cell* **112**, 453–465. (doi:10.1016/S0092-8674(03)00120-X)

37. Gerisch G, Bretschneider T, Müller-Taubenberger A, Simmeth E, Ecke M, Diez S, Anderson K. 2004 Mobile actin clusters and traveling waves in cells recovering from actin depolymerization. *Biophys. J.* **87**, 3493–3503. (doi:10.1529/biophysj.104.047589)

38. Lemieux MG, Janzen D, Hwang R, Roldan J, Jarchum I, Knecht DA. 2014 Visualization of the actin cytoskeleton: different F-actin-binding probes tell different stories. *Cytoskeleton* **71**, 157–169. (doi:10.1002/cm.21160)

39. Small JV. 2015 Pushing with actin: from cells to pathogens. *Biochem. Soc. Trans.* **43**, 84–91. (doi:10.1042/BST20140184)

40. Theriot JA, Mitchison TJ, Tilney LG, Portnoy DA. 1992 The rate of actin-based motility of intracellular *Listeria monocytogenes* equals the rate of actin polymerization. *Nature* **357**, 257–260. (doi:10.1038/357257a0)

41. Bernheim-Groswasser A, Wiesner S, Golsteyn RM, Carlier M-F, Sykes C. 2002 The dynamics of actin-based motility depend on surface parameters. *Nature* **417**, 308–311. (doi:10.1038/417308a)

42. Zhu J, Mogilner A. 2012 Mesoscopic model of actin-based propulsion. *PLoS Comput. Biol.* **8**, e1002764. (doi:10.1371/journal.pcbi.1002764)

43. Mogilner A, Oster G. 1996 Cell motility driven by actin polymerization. *Biophys. J.* **71**, 3030–3045. (doi:10.1016/S0006-3495(96)79496-1)

44. Vicker MG. 2000 Reaction-diffusion waves of actin filament polymerization/depolymerization in *Dictyostelium* pseudopodium extension and cell locomotion. *Biophys. Chem.* **84**, 87–98. (doi:10.1016/S0301-4622(99)00146-5)

45. Pollitt AY, Insall RH. 2009 WASP and SCAR/WAVE proteins: the drivers of actin assembly. *J. Cell Sci.* **122**, 2575–2578. (doi:10.1242/jcs.023879)

46. Cai L, Makhov AM, Schafer DA, Bear JE. 2008 Coronin 1B antagonizes cortactin and remodels Arp2/3-containing actin branches in lamellipodia. *Cell* **134**, 828–842. (doi:10.1016/j.cell.2008.06.054)

47. Taniguchi D, Ishihara S, Oonuki T, Honda-Kitahara M, Kaneko K, Sawai S. 2013 Phase geometries of two-dimensional excitable waves govern self-organized morphodynamics of amoeboid cells. *Proc. Natl Acad. Sci. USA* **110**, 5016–5021. (doi:10.1073/pnas.1218025110)

48. Xiong D, Xiao S, Guo S, Lin Q, Nakatsu F, Wu M. 2016 Frequency and amplitude control of cortical oscillations by phosphoinositide waves. *Nat. Chem. Biol.* **12**, 159–166. (doi:10.1038/nchembio.2000)

49. Enculescu M, Sabouri-Ghomi M, Danuser G, Falcke M. 2010 Modeling of protrusion phenotypes driven by the actin-membrane interaction. *Biophys. J.* **98**, 1571–1581. (doi:10.1016/j.bpj.2009.12.4311)

50. Doubrovinski K, Kruse K. 2011 Cell motility resulting from spontaneous polymerization waves. *Phys. Rev. Lett.* **107**, 258103. (doi:10.1103/PhysRevLett.107.258103)

51. Carlsson AE. 2010 Dendritic actin filament nucleation causes traveling waves and patches. *Phys. Rev. Lett.* **104**, 228102. (doi:10.1103/PhysRevLett.104.228102)

52. Danuser G, Allard J, Mogilner A. 2013 Mathematical modeling of eukaryotic cell migration: insights beyond experiments. *Ann. Rev. Cell Dev. Biol.* **29**, 501–528. (doi:10.1146/annurev-cellbio-101512-122308)

53. Hoeller O, Kay RR. 2007 Chemotaxis in the absence of PIP3 gradients. *Curr. Biol.* **17**, 813–817. (doi:10.1016/j.cub.2007.04.004)

54. Sun X, Driscoll MK, Guven C, Das S, Parent CA, Fourkas JT, Losert W. 2015 Asymmetric nanotopography biases cytoskeletal dynamics and promotes unidirectional cell guidance. *Proc. Natl Acad. Sci. USA* **112**, 12 557–12 562. (doi:10.1073/pnas.1502970112)

55. Yan J, Mihaylov V, Xu X, Brzostowski JA, Li H, Liu L, Veenstra TD, Parent CA, Jin T. 2012 A Gβγ effector, ElmoE, transduces GPCR signaling to the actin network during chemotaxis. *Dev. Cell* **22**, 92–103. (doi:10.1016/j.devcel.2011.11.007)

56. Lockley R, Ladds G, Bretschneider T. 2015 Image based validation of dynamical models for cell reorientation. *Cytomet. A* **87**, 471–480. (doi:10.1002/cyto.a.22600)

57. Levchenko A, Iglesias PA. 2002 Models of eukaryotic gradient sensing: application to chemotaxis of amoebae and neutrophils. *Biophys. J.* **82**, 50–63. (doi:10.1016/S0006-3495(02)75373-3)

58. Elliott CM, Stinner B, Venkataraman C. 2012 Modelling cell motility and chemotaxis with evolving surface finite elements. *J. R. Soc. Interface* **9**, 3027–3044. (doi:10.1098/rsif.2012.0276)

59. Neilson MP, Veltman DM, van Haastert PJM, Webb SD, Mackenzie JA, Insall RH. 2011 Chemotaxis: a feedback-based computational model robustly predicts multiple aspects of real cell behaviour. *PLoS Biol.* **9**, e1000618 (doi:10.1371/journal.pbio.1000618)

60. Binamé F, Pawlak G, Roux P, Hibner U. 2010 What makes cells move: requirements and obstacles for spontaneous cell motility. *Mol. BioSyst.* **6**, 648–661. (doi:10.1039/b915591k)

61. Renkawitz J, Sixt M. 2010 Mechanisms of force generation and force transmission during interstitial leukocyte migration. *EMBO Rep.* **11**, 744–750. (doi:10.1038/embor.2010.147)

62. Zatulovskiy E, Tyson R, Bretschneider T, Kay RR. 2014 Bleb-driven chemotaxis of *Dictyostelium* cells. *J. Cell Biol.* **204**, 1027–1044. (doi:10.1083/jcb.201306147)

63. Barry NP, Bretscher MS. 2010 *Dictyostelium* amoebae and neutrophils can swim. *Proc. Natl Acad. Sci. USA* **107**, 11 376–11 380. (doi:10.1073/pnas.1006327107)

64. Van Haastert PJM. 2011 Amoeboid cells use protrusions for walking, gliding and swimming. *PLoS ONE* **6**, e27532. (doi:10.1371/journal.pone.0027532)

65. Wang Q, Othmer HG. 2015 Computational analysis of amoeboid swimming at low Reynolds number. *J. Math. Biol.* **72**, 1893–1926. (doi:10.1007/s00285-015-0925-9)

66. Weijer CJ. 2004 *Dictyostelium* morphogenesis. *Curr. Opin. Genetics Dev.* **14**, 392–398. (doi:10.1016/j.gde.2004.06.006)

67. Kessin RH. 2001 *Dictyostelium: evolution, cell biology, and the development of multicellularity*, vol. 38. Cambridge, UK: Cambridge University Press.

68. Dormann D, Weijer CJ. 2006 Imaging of cell migration. *EMBO J.* **25**, 3480–3493. (doi:10.1038/sj.emboj.7601227)

69. Devreotes P, Horwitz AR. 2015 Signaling networks that regulate cell migration. *Cold Spring Harb. Perspect. Biol.* **7**, a005959. (doi:10.1101/cshperspect.a005959)

70. Shi C, Huang C-H, Devreotes PN, Iglesias PA. 2013 Interaction of motility, directional sensing, and polarity modules recreates the behaviors of chemotaxing cells. *PLoS Comput. Biol.* **9**, e1003122. (doi:10.1371/journal.pcbi.1003122)

71. Gerisch G, Hulser D, Malchow D, Wick U. 1975 Cell communication by periodic cyclic camp pulses. *Phil. Trans. R. Soc. Lond.* **272**, 181–192. (doi:10.1098/rstb.1975.0080)

72. Dinauer MC, Steck TL, Devreotes PN. 1980 Cyclic 3′,5′ AMP relay in *Dictyostelium discoideum* IV. Recovery of the cAMP signaling response after adaptation to cAMP. *J. Cell Biol.* **86**, 545–553. (doi:10.1083/jcb.86.2.545)

73. Garcia GL, Parent CA. 2008 Signal relay during chemotaxis. *J. Microsc.* **231**, 529–534. (doi:10.1111/j.1365-2818.2008.02066.x)

74. Martiel J-L, Goldbeter A. 1987 A model based on receptor desensitization for cyclic AMP signaling in *Dictyostelium* cells. *Biophys. J.* **52**, 807–828. (doi:10.1016/S0006-3495(87)83275-7)

75. Othmer HG, Monk PB, Rapp PE. 1985 A model for signal relay and adaptation in *Dictyostelium discoideum*. Part II. Analytical and numerical results. *Math. Biosci.* **77**, 77–139. (doi:10.1016/0025-5564(85)90092-6)

76. Winfree AT. 1972 Spiral waves of chemical activity. *Science* **175**, 634–636. (doi:10.1126/science.175.4022.634)

77. Alcantara F, Monk M. 1974 Signal propagation during aggregation in the slime mold *Dictyostelium discoideum*. *J. Gen. Microbiol.* **85**, 321–334. (doi:10.1099/00221287-85-2-321)

78. Durston AJ. 1974 Pacemaker activity during aggregation in *Dictyostelium discoideum*. *Dev. Biol.* **37**, 225–235. (doi:10.1016/0012-1606(74)90144-4)

79. Siegert F, Weijer CJ. 1989 Digital image processing of optical density wave propagation in *Dictyostelium discoideum* and analysis of the effects of caffeine and ammonia. *J. Cell Sci.* **93**, 325–335.

80. Palsson E, Cox EC. 1996 Origin and evolution of circular waves and spirals in *Dictyostelium discoideum* territories. *Proc. Natl Acad. Sci. USA* **93**, 1151–1155. (doi:10.1073/pnas.93.3.1151)

81. Pate E, Othmer HG. 1986 Differentiation, cell sorting and proportion regulation in the slug stage of *Dictyostelium discoideum*. *J. Theor. Biol.* **118**, 301–319. (doi:10.1016/S0022-5193(86)80061-3)

82. Othmer HG, Pate EF. 1987 A model for pattern formation in *Dictyostelium discoideum*. In *Mathematical topics in population biology, morphogenesis, and neurosciences* (eds E Teramoto, M Yamaguti), pp. 224–233. Berlin, Germany: Springer.

83. Levine H, Reynolds W. 1991 Streaming instability of aggregating slime mold amoebae. *Phys. Rev. Lett.* **66**, 2400–2403. (doi:10.1103/PhysRevLett.66.2400)

84. Van Oss C, Panfilov AV, Hogeweg P, Siegert F, Weijer CJ. 1996 Spatial pattern formation during aggregation of the slime mould *Dictyostelium discoideum*. *J. Theor. Biol.* **181**, 203–213. (doi:10.1006/jtbi.1996.0126)

85. Vasiev B, Siegert F, Weijer CJ. 1997 A hydrodynamic model for *Dictostelium discoideum* mound formation. *J. Theor. Biol.* **184**, 441–450. (doi:10.1006/jtbi.1996.0282)

86. Noorbakhsh J, Schwab DJ, Sgro AE, Gregor T, Mehta P. 2015 Modeling oscillations and spiral waves in *Dictyostelium* populations. *Phys. Rev. E* **91**, 062711. (doi:10.1103/PhysRevE.91.062711)

87. Gregor T, Fujimoto K, Masaki N, Sawai S. 2010 The onset of collective behavior in social amoebae. *Science* **328**, 1021–1025. (doi:10.1126/science.1183415)

88. Sgro AE, Schwab DJ, Noorbakhsh J, Mestler T, Mehta P, Gregor T. 2015 From intracellular signaling to population oscillations: bridging size- and time-

scales in collective behavior. *Mol. Syst. Biol.* **11**, 779. (doi:10.15252/msb.20145352)

89. Harloff C, Gerisch G, Noegel AA. 1989 Selective elimination of the contact site A protein of *Dictyostelium discoideum* by gene disruption. *Genes Dev.* **3**, 2011–2019. (doi:10.1101/gad.3.12a.2011)

90. Kriebel PW, Parent CA. 2009 Group migration and signal relay in *Dictyostelium*. In *Chemotaxis*, pp. 111–124. Berlin, Germany: Springer.

91. Rietdorf J, Siegert F, Weijer CJ. 1996 Analysis of optical density wave propagation and cell movement during mound formation in *Dictyostelium discoideum*. *Dev. Biol.* **177**, 427–438. (doi:10.1006/dbio.1996.0175)

92. Vicker MG. 2002 F-actin assembly in *Dictyostelium* cell locomotion and shape oscillations propagates as a self-organized reaction–diffusion wave. *FEBS Lett.* **510**, 5–9. (doi:10.1016/S0014-5793(01)03207-0)

93. del Alamo JC, Meili R, Alonso-Latorre B, Rodrguez-Rodrguez J, Aliseda A, Firtel RA, Lasheras JC. 2007 Spatio-temporal analysis of eukaryotic cell motility by improved force cytometry. *Proc. Natl Acad. Sci. USA* **104**, 13 343–13 348. (doi:10.1073/pnas.0705815104)

94. Bastounis E, Meili R, Álvarez-González B, Francois J, del Álamo JC, Firtel RA, Lasheras JC. 2014 Both contractile axial and lateral traction force dynamics drive amoeboid cell motility. *J. Cell Biol.* **204**, 1045–1061. (doi:10.1083/jcb.201307106)

95. Alvarez-Gonzalez B, Meili R, Bastounis E, Firtel RA, Lasheras JC, del Álamo JC. 2015 Three-dimensional balance of cortical tension and axial contractility enables fast amoeboid migration. *Biophys. J.* **108**, 821–832. (doi:10.1016/j.bpj.2014.11.3478)

96. Wong E, Yang C, Wang J, Fuller D, Loomis WF, Siu C-H. 2002 Disruption of the gene encoding the cell adhesion molecule ddCAD-1 leads to aberrant cell sorting and cell-type proportioning during *Dictyostelium* development. *Development* **129**, 3839–3850.

97. Benabentos R *et al.* 2009 Polymorphic members of the lag gene family mediate kin discrimination in *Dictyostelium*. *Curr. Biol.* **19**, 567–572. (doi:10.1016/j.cub.2009.02.037)

98. Parkinson K, Bolourani P, Traynor D, Aldren NL, Kay RR, Weeks G, Thompson CR. 2009 Regulation of rap1 activity is required for differential adhesion, cell-type patterning and morphogenesis in *Dictyostelium*. *J. Cell Sci.* **122**, 335–344. (doi:10.1242/jcs.036822)

99. Matsukuma S, Durston AJ. 1979 Chemotactic cell sorting in *Dictyostelium discoideum*. *J. Embryol. Exp. Morphol.* **50**, 243–251.

100. Sternfeld J, David CN. 1981 Cell sorting during pattern formation in *Dictyostelium*. *Differentition* **20**, 10–21. (doi:10.1111/j.1432-0436.1981.tb01150.x)

101. Traynor D, Kessin RH, Williams JG. 1992 Chemotactic sorting to cAMP in the multicellular stage of *Dictyostelium discoideum* development. *Proc. Natl Acad. Sci. USA* **89**, 8303–8307. (doi:10.1073/pnas.89.17.8303)

102. Springer M, Patterson B, Spudich J. 1994 Stage-specific requirement for myosin II during *Dictyostelium* development. *Development* **120**, 2651–2660.

103. Moores SL, Sabry JH, Spudich JA. 1996 Myosin dynamics in live *Dictyostelium* cells. *Proc. Natl Acad. Sci. USA* **93**, 443–446. (doi:10.1073/pnas.93.1.443)

104. Clow PA, Chen T, Chisholm RL, McNally JG. 2000 Three-dimensional *in vivo* analysis of Dictyostelium mounds reveals directional sorting of prestalk cells and defines a role for the myosin II regulatory light chain in prestalk cell sorting and tip protrusion. *Development* **127**, 2715–2728.

105. van Wijk IV, Fukuzawa M, Devreotes PN, Schaap P. 2001 Adenylyl cyclase A expression is tip-specific in *Dictyostelium* slugs and directs statA nuclear translocation and cudA gene expression. *Dev. Biol.* **234**, 151–160. (doi:10.1006/dbio.2001.0232)

106. Steinbock O, Siegert F, Muller SC, Weijer CJ. 1993 Three-dimensional waves of excitation during *Dictyostelium* morphogenesis. *Proc. Natl Acad. Sci. USA* **90**, 7332–7335. (doi:10.1073/pnas.90.15.7332)

107. Bretschneider T, Siegert F, Weijer CJ. 1995 Three-dimensional scroll waves of cAMP could direct cell movement and gene expression in Dictyostelium slugs. *Proc. Natl Acad. Sci. USA* **92**, 4387–4391. (doi:10.1073/pnas.92.10.4387)

108. Patel H, Guo K, Parent C, Gross J, Devreotes PN, Weijer CJ. 2000 A temperature-sensitive adenylyl cyclase mutant of *Dictyostelium*. *EMBO J.* **19**, 2247–2256. (doi:10.1093/emboj/19.10.2247)

109. Morrison A, Blanton RL, Grimson M, Fuchs M, Williams K, Williams J. 1994 Disruption of the gene encoding the ecmA, extracellular matrix protein of *Dictyostelium* alters slug morphology. *Dev. Biol.* **163**, 457–466. (doi:10.1006/dbio.1994.1162)

110. Blanton RL, Fuller D, Iranfar N, Grimson MJ, Loomis WF. 2000 The cellulose synthase gene of *Dictyostelium*. *Proc. Natl Acad. Sci. USA* **97**, 2391–2396. (doi:10.1073/pnas.040565697)

111. Tsujioka M, Yoshida K, Inouye K. 2004 Talin B is required for force transmission in morphogenesis of *Dictyostelium*. *EMBO J.* **23**, 2216–2225. (doi:10.1038/sj.emboj.7600238)

112. Bukharova T, Weijer G, Bosgraaf L, Dormann D, van Haastert P, Weijer C. 2005 Paxillin is required for cell-substrate adhesion, cell sorting and slug migration during *Dictyostelium* development. *J. Cell Sci.* **118**, 4295–4310. (doi:10.1242/jcs.02557)

113. Rieu J-P, Barentin C, Maeda Y, Sawada Y. 2005 Direct mechanical force measurements during the migration of *Dictyostelium* slugs using flexible substrata. *Biophys. J.* **89**, 3563–3576. (doi:10.1529/biophysj.104.056333)

114. Rieu J-P, Saito T, Delanoë-Ayari H, Sawada Y, Kay RR. 2009 Migration of *Dictyostelium* slugs: anterior-like cells may provide the motive force for the prespore zone. *Cell Motil. Cytoskelet.* **66**, 1073–1086. (doi:10.1002/cm.20411)

115. Rieu J-P, Delanoë-Ayari H. 2012 Shell tension forces propel *Dictyostelium* slugs forward. *Phys. Biol.* **9**, 066001. (doi:10.1088/1478-3975/9/6/066001)

116. Odell GM, Bonner JT. 1986 How the *Dictyostelium discoideum* grex crawls. *Phil. Trans. R. Soc. Lond. B* **312**, 487–525. (doi:10.1098/rstb.1986.0016)

117. Vasiev B, Weijer CJ. 2003 Modelling of *Dictyostelium discoideum* slug migration. *J. Theor. Biol.* **223**, 347–359. (doi:10.1016/S0022-5193(03)00103-6)

118. Dallon JC, Othmer HG. 2004 How cellular movement determines the collective force generated by the *Dictyostelium discoideum* slug. *J. Theor. Biol.* **231**, 203–222. (doi:10.1016/j.jtbi.2004.06.015)

119. Dormann D, Siegert F, Weijer CJ. 1996 Analysis of cell movement during the culmination phase of *Dictyostelium* development. *Development* **122**, 761–769.

120. Sternfeld J. 1998 The anterior-like cells in *Dictyostelium* are required for the elevation of the spores during culmination. *Dev. Genes Evol.* **208**, 487–494. (doi:10.1007/s004270050207)

121. Marée AF, Hogeweg P. 2001 How amoeboids self-organize into a fruiting body: multicellular coordination in *Dictyostelium discoideum*. *Proc. Natl Acad. Sci. USA* **98**, 3879–3883. (doi:10.1073/pnas.061535198)

122. Maree AF, Hogeweg P. 2002 Modelling *Dictyostelium discoideum* morphogenesis: the culmination. *Bull. Math. Biol.* **64**, 327–353. (doi:10.1006/bulm.2001.0277)

123. Sternfeld J, David CN. 1982 Fate and regulation of anterior-like cells in *Dictyostelium* slugs. *Dev. Biol.* **93**, 111–118. (doi:10.1016/0012-1606(82)90244-5)

124. Ràfols I, Sawada Y, Amagai A, Maeda Y, MacWilliams HK. 2001 Cell type proportioning in *Dictyostelium* slugs: lack of regulation within a 2.5-fold tolerance range. *Differentiation* **67**, 107–116. (doi:10.1046/j.1432-0436.2001.670403.x)

125. Schaap P, Tang Y, Othmer HG. 1996 A model for pattern formation in *Dictyostelium discoideum*. *Differentiation* **60**, 1–16. (doi:10.1046/j.1432-0436.1996.6010001.x)

126. Pineda M, Weijer C, Eftimie R. 2015 Modelling cell movement, cell differentiation, cell sorting and proportion regulation in *Dictyostelium discoideum* aggregations. *J. Theor. Biol.* **370**, 135–150. (doi:10.1016/j.jtbi.2015.01.042)

127. Bonner JT. 1974 *On development; the biology of form*. Cambridge, MA: Harvard University Press.